NBSIR 85-3196

Slide-Rule Estimates of Fire Growth

J. R. Lawson
J. G. Quintiere

U.S. DEPARTMENT OF COMMERCE
National Bureau of Standards
National Engineering Laboratory
Center for Fire Research
Gaithersburg, MD 20899

June 1985

Supported in part by:
U.S. David Taylor Naval Ship
rch and Development Center
ngton, DC

NBSIR 85-3196

SLIDE-RULE ESTIMATES OF FIRE GROWTH

J. R. Lawson
J. G. Quintiere

U.S. DEPARTMENT OF COMMERCE
National Bureau of Standards
National Engineering Laboratory
Center for Fire Research
Gaithersburg, MD 20899

June 1985

Supported in part by:
U.S. David Taylor Naval Ship
Research and Development Center
Washington, DC

U.S. DEPARTMENT OF COMMERCE, Malcolm Baldrige, *Secretary*
NATIONAL BUREAU OF STANDARDS, Ernest Ambler, *Director*

Table of Contents

List of Tables

List of Figures

SLIDE-RULE ESTIMATES OF FIRE GROWTH

by

J.R. Lawson and J.G. Quintiere

Abstract

A series of prediction methods have been assembled to provide an analytical basis for estimating fire growth in compartmens. Solutions for each prediction method can be made using programmable scientific calculators. Prediction methods are presented for: fire size and growth rates, mass loss rates, radiant heat flux, flame height, radial flame impingement, heat flux to a ceiling, smoke filling of a room, carbon monoxide hazard with smoldering fires, temperature rise in a compartment, ventilation flow rate, flashover ocurrence, corridor smoke transfer and filling, smoke concentration, visibility, flame spread rates, and fire burn time.

These predictive methods are useful for estimating many of the critical elements related to fire behavior and help provide a better understanding of this complex phenomenon.

This report appears as Appendix B in Fire Growth in Combat Ships by J.G. Quintiere, H.R. Baum and J.R. Lawson, NBSIR 85-3159.

Key words: Calculators; computer programs; fire growth; fire models; room fires.

1. Introduction

The purpose of this paper is to provide an analytical basis for estimating the growth of fire in compartments and its consequences. All prediction methods have been selected to allow for solutions to be made using programmable scientific calculators or pocket computers. The paper consists of a series of equations or data each of which describes a particular process in a fire's growth. Only minor discussions of theory are presented to provide some understanding of concepts related to the problem in question. For more information on each process discussed, refer to the appropriate reference materials. The equations presented will apply only to specific fuels or conditions and hence will be approximate when used for more complex or different situations. Also, any consideration of these equations as constituting a dynamic interacting fire system will be filled with inconsistencies. Nevertheless, this series of equations can provide a reasonable sense of the quantitative features of fire growth. It will relate to material type - solids or liquids - not specific materials. For specific materials other than those addressed in the text, one would have to acquire data that is unique to the materials being studied. Moreover, the state-of-the-art does not fully allow for fire predictions of specific materials.

2. Fire Size and Growth Rates

In order to make fire growth predictions, one must make a basic assumption about what material is burning. This assumption is used to calculate an estimated burning rate for the model and is a key factor for calculating other

fire characteristics associated with fire growth. The four basic types of fuels identified with fire are usually classed as:

A. Solids (non-metals)
B. Liquids
C. Electrical Equipment
D. Metals

In this paper we shall consider only some representative ways of estimating Class A and Class B materials. For Class A we will consider first a wood crib as representative of a complex structure; then a solid surface like a mattress, chair or slab of material. For Class B materials, a method for estimating burning rates is suggested and input data will be provided for some common liquid fuels.

In 1976, Delichatosios reported work accomplished on the study of fire growth in wood cribs [1]. In his work, it was shown that a simple model could be used to predict fire growth rates for wood cribs. This model is put to use in this report for the same purpose. The model pays particular attention to crib geometry, surface area exposed for burning, and the wood's thermal properties. The equation used for estimating burning rate, $\dot{m}_f$, for cribs ignited in the center is,

BURNING RATES FOR WOOD CRIBS.

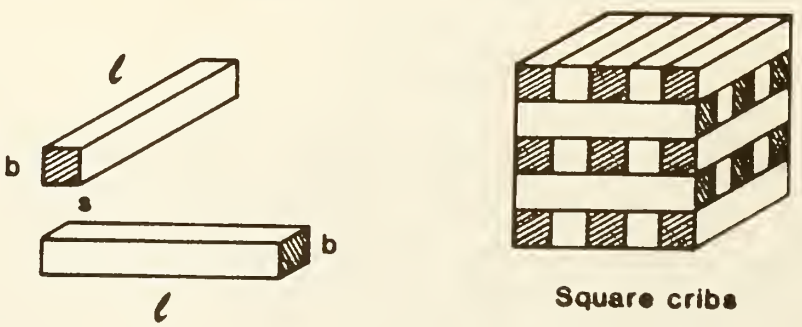

Figure B1. Sketch of a Wood Crib.

$$\dot{m}_f = \dot{m}'' A_s \frac{\pi}{2} \left(\frac{t}{t_o}\right)^2 \quad \text{for } t \leq t_o \tag{1}$$

$\dot{m}''$ - specific burning rate found by: $\dot{m}'' = cb^{-1/2} f(P)$ where

$c \sim 10^{-3}$ g/cm$^{3/2}$ · s

b - wood stick thickness (cm)

f(P) - found in Figure B2

$P = A_v s^{1/2} b^{1/2} A_s$

A_s - total exposed surface area of wood in the crib = $4\ell bnN$ where

ℓ - stick length (cm)

s - stick spacing (cm) = $\ell - nb$

n - sticks per crib layer

N - layers of sticks in crib

A_v - total shaft cross-sectional area = $s^2 \cdot$ (number = $(n-1)^2$) of shafts)

t - time in seconds

t_o - time for flames to spread to the outer edge of crib = $n/(\sqrt{2}\ \xi)$

$\xi \sim 0.045\ s^{-1}$

$$\dot{m}_f = A_s c b^{-1/2} f(P) \text{ for } t > t_o \qquad (2)$$

where f(P) is plotted in Figure B2 and when $P > 0.07$, $f(P) = 1$.

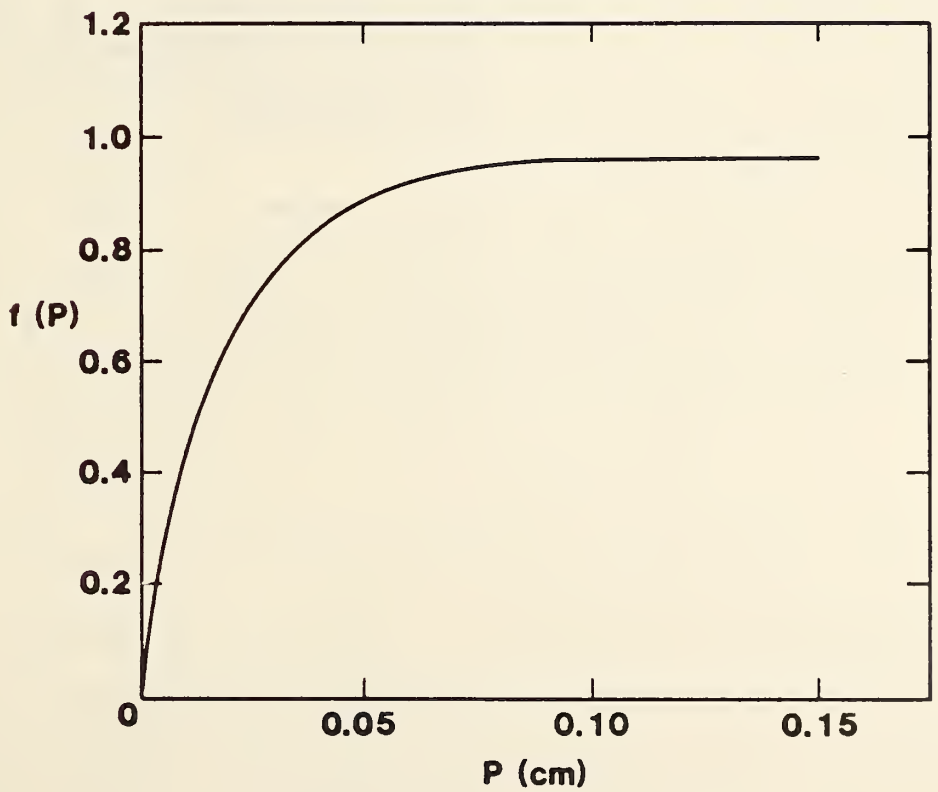

Figure B2. Reduced specific burning rate as a function of the crib porosity for ponderosa pine wood cribs (taken from Heskestad) [2].

BURNING RATES FOR FURNISHINGS. With more complex solids like furnishings, representative data is drawn from a report by Lawson, et al. [3]. Figure B3 exhibits the mass loss rate for a typical stuffed chair and Figure B4 provides data on a typical three seat sofa. Mass loss rate data for burning mattresses is obtained from a report published in 1977 by Babrauskas [4]. Figure B5 presents data for cotton and mixed fiber core mattress specimens. Data from these and other reports can be substituted in for calculations on burning rates for furnishings. Furnishings are complex solids that do not currently lend themselves to simple fire modeling, other common solid materials do.

BURNING RATES FOR PLASTIC POOL FIRES. The burning rate for polyurethane foam was estimated with the following pool fire model developed by Orloff [5].

$$\dot{m}_f = \alpha e^{(\alpha t - \beta)} \text{ g/s} \qquad (3)$$

where $\alpha = 0.033 s^{-1}$

β = 1.29 (corresponds to a time shift of 30.35 which accounts for a particular ignition character in this experiment)

t = time in seconds

for the period $80 < t < 170$ s.

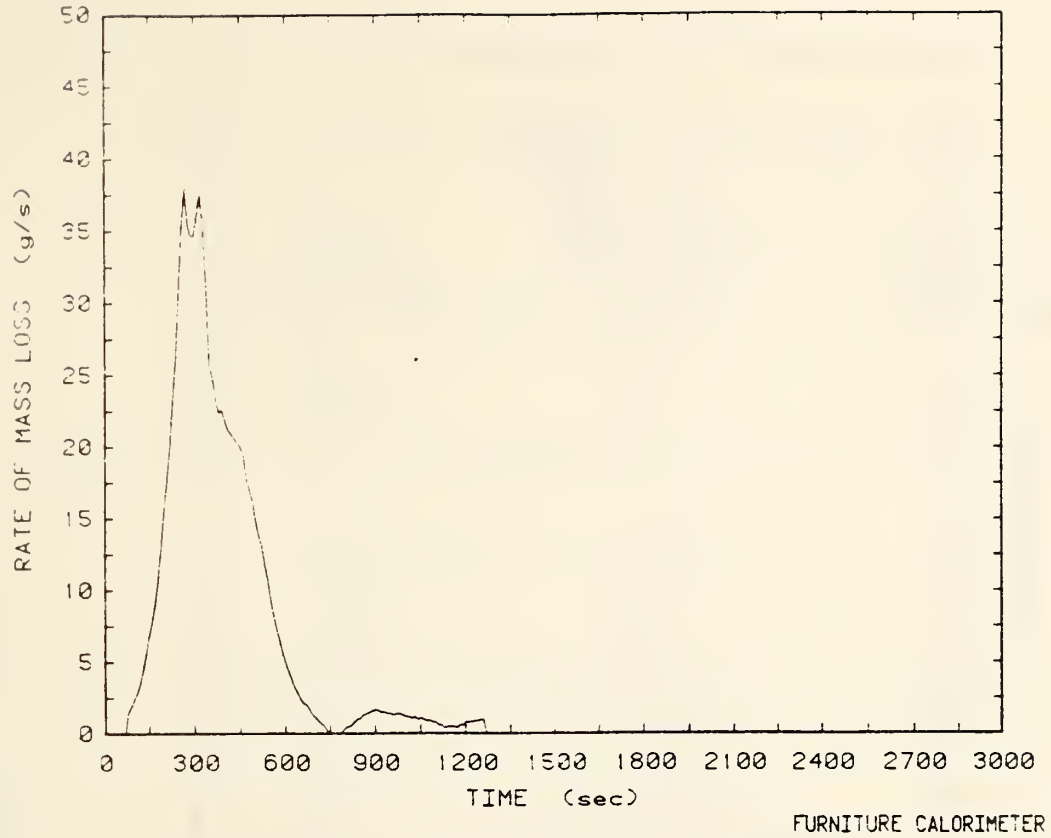

Figure B3. Rate of mass loss plot for easy chair [3].

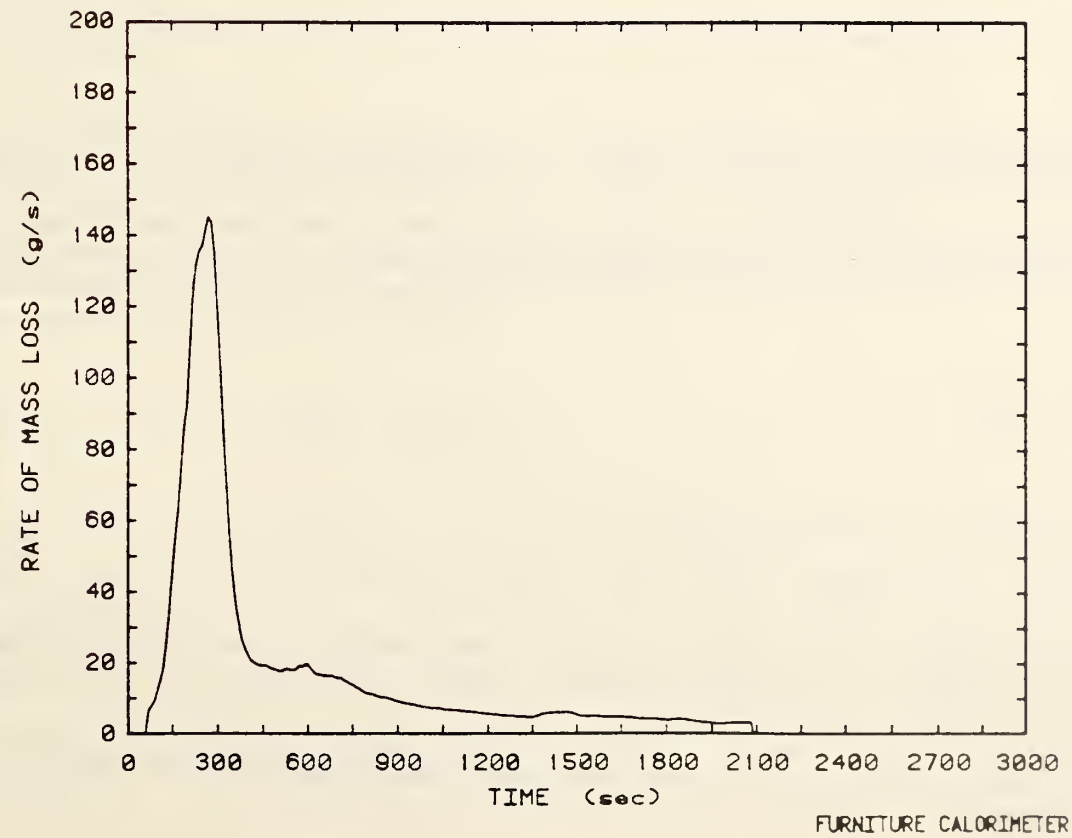

Figure B4. Rate of mass loss plot for sofa with "California foam" cushions [3].

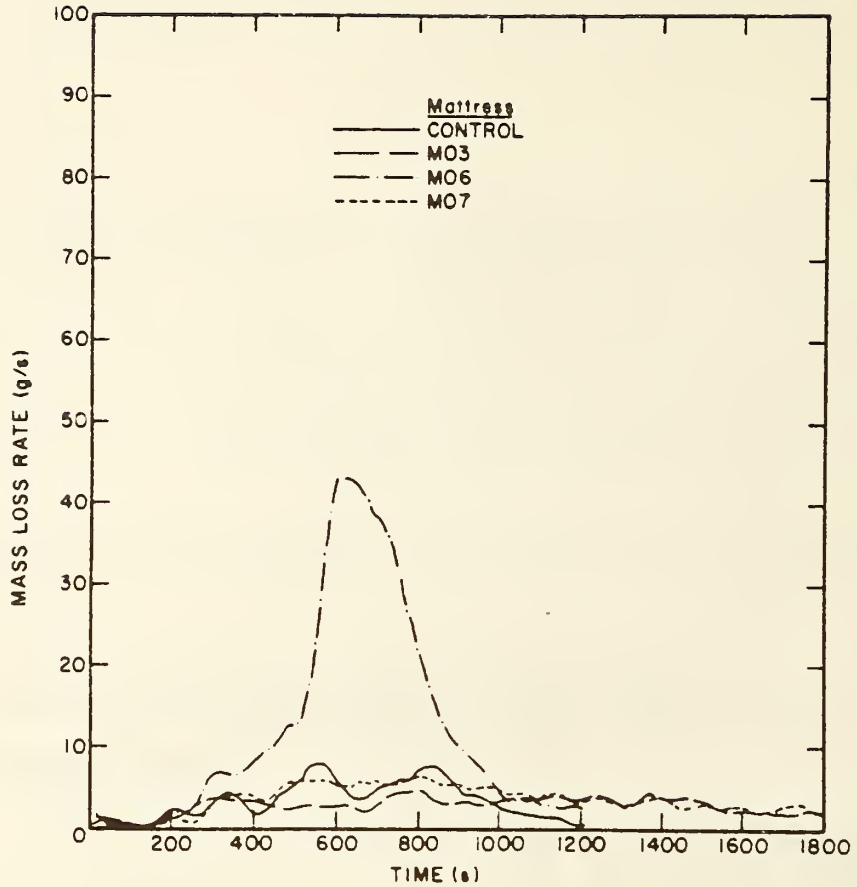

Figure B5. Weight loss for cotton and mixed fiber core specimens [4].

A review of data from furniture fires [3] indicates that for polyurethane foam chairs, Eq. (3) may also produce useful estimates for t > 170 s.

Modak and Croce [6] studied the burning of polymethyl methacrylate (PMMA) plastic pool fires and found that experimentally measured burning rates per unit area, $\dot{m}''(t)$, at time t after ignition were correlated by the equation:

$$\frac{\dot{m}_s'' - \dot{m}''(t)}{\dot{m}_s'' - \dot{m}_i''} = e^{-t/\tau} \qquad (4)$$

Therefore $\dot{m}''(t)$ can be estimated by,

$$\dot{m}''(t) = -\left[e^{-t/\tau}(\dot{m}_s'' - m_i'') - \dot{m}_s''\right] \qquad (5)$$

where $\dot{m}_i'' \cong 4$ g/m^{2}s is the average burning rate per unit area; $\dot{m}_s''$ is the steady burning rate, and τ is the characteristic "gasification time" to reach steady state.

Table B1 contains data that can be used for calculating $\dot{m}''(t)$ for various size pools of PMMA.

Table B1

Results for PMMA Pool Fires of Varying Scale [6]

Pool area m^2	Measured steady burning rate per unit area $\dot{m}''_s$ $(g/m^2 s)$	Gasification time parameter[b] τ (s)	Radiative fraction of total heat release rate χ (-)
2.58×10^{-3}	4.6	NA	0.28[c]
5.81×10^{-3}	5.6	NA	0.32[c]
0.0232	7.7[b]	3448	0.32[c]
0.0523	9.0[b]	1587	0.42
0.0929	17.4[b]	1136	0.42
0.3716	18.0	500	0.42
0.5806	18.25	357	0.42
1.4865	20.0	118	0.42

[b]Best fit.

[c]Varied with time.

NA not available.

BURNING RATES FOR LIQUID POOL FIRES. In order to estimate burning rates for liquid pool fires, data were taken from a report by Burgess, et al. [7]. Their study shows the burning rate for a number of liquid fuels is a function of pool diameter. But for large diameter pools, flame radiation dominates and a maximum burning rate is achieved. Empirically they suggest that this maximum burning rate can be found by

$$\dot{m}''_{max} = 6.5 \times 10^{-3} \frac{cm}{min} \rho \Delta H_c / \Delta H_v \qquad (6)$$

where ρ is the liquid density

ΔH_c is the heat of combustion, and

ΔH_v is the heat of vaporization.

Some specific results are given below in Table B2 for pool diameters greater than 1.5 m.

Table B2

Burning Rates for Liquid Pool Fires.

Liquid	$\dot{m}''_{max}$ (g/m²s)	x_r, flame radiation fraction (%)
n-Hexane	76.9	42
Benzene	87.9	35
UDMH	44.3	24
Methanol	15.8	15
Gasoline	45.	-
Diesel fuel	43.	-

3. Radiant Heat Flux to a Target

After the initial fire has been defined, it is important to know something about the heat radiated from the source that could cause secondary ignitions. A technique discussed by Modak [8] will be used to estimate radiant flux. This method is depicted in the sketch below and is detailed in Eq. (7).

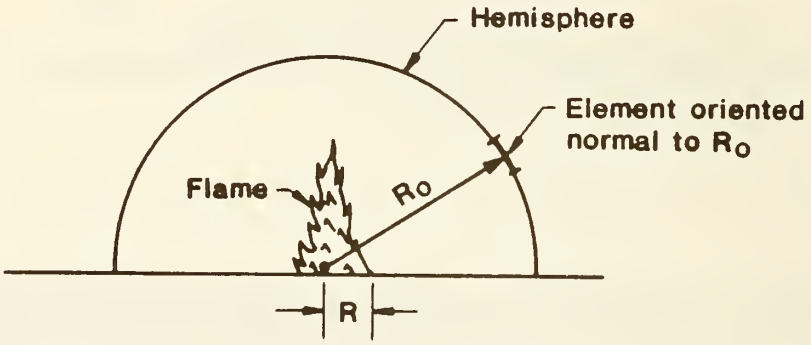

Figure B6. Fire radiant heat transfer to a target.

The incident heat flux at a target can be approximated as

$$\dot{q}''_o \cong P/4\pi R_o^2 \qquad (7)$$

where P is the total radiative power output of the flame. P can be represented as $\chi_r \dot{Q}$ where χ_r is the radiative fraction and $\dot{Q}$ is total energy release rate. Usually χ_r ranges from 20 to 45 percent for many fuels. For a typical pool fire Modak[8] finds that the above formula is > 90 percent accurate when $R_o/R > 4$. At $R_o/R = 2$, the approximation is about 80 percent correct.

4. Flame Height

Since burning rates and thermal radiation to targets have been defined, a third physical phenomenon relating to flame geometry must be considered. Flame height is an important characteristic which provides information needed for estimating heat transfer to a room's ceiling and other structures that may be located above a fire. It has been shown by McCaffrey [9] that flame height, Z_f, is related to the total energy release rate, $\dot{Q}$, and the diameter, D, of the fire base. This is illustrated in Figure B7 which is taken from a report by Zukoski, et al. [10].

For flame heights where $(Z_f/D) > 2$, Zukoski suggested the following equation which provides a reasonable estimate:

$$Z_f = [0.23 \text{ m/kW}^{2/5}] \dot{Q}^{2/5}, \tag{8}$$

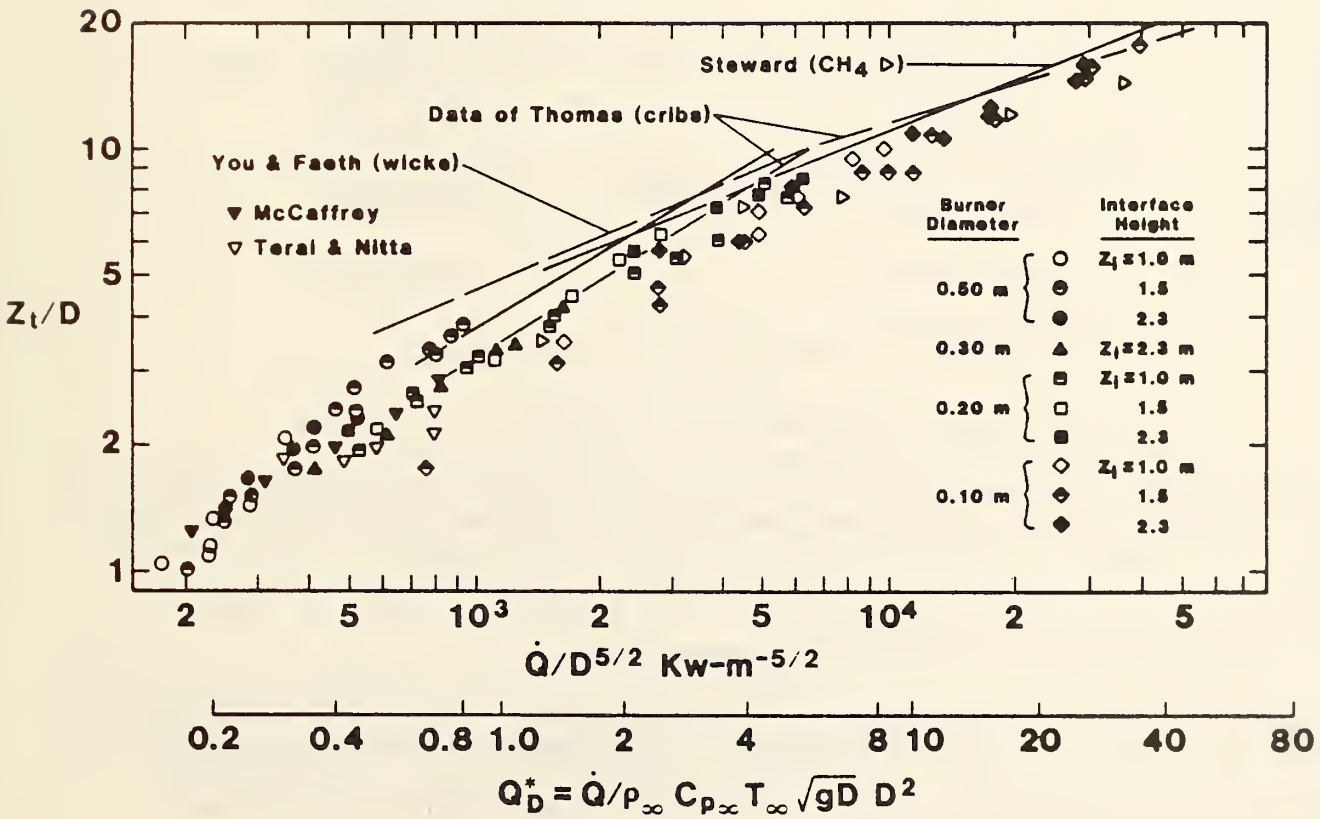

Figure B7. Flame height dependence on heat release parameters [10].

or use Figure B7 directly.

In addition, work reported by Hasemi and Tokunaga [11] for a 0.5 m diameter burner showed that the height of the continuous flame region could be estimated by

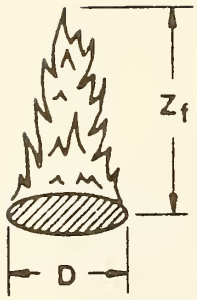

$$Z_{f\ min} = (0.11\ m/kW^{2/5})\ \dot{Q}^{2/5} \quad (9)$$

and the height to the flame tip could be estimated by

$$Z_{f\ max} = (0.21\ m/kW^{2/5})\ \dot{Q}^{2/5} \quad (10)$$

Figure B8a. For Open Flames

These results are consistent with Eq. (8) and Figure B7, but explicitly address the variation of the flame structure from a continuous luminous region to a region above which is intermittent flames terminating at the flame "tip".

Their work also provides equations that are useful in estimating flame heights in a corner fire scenario. See Figure B8b. Equations (11) and (12) provide these estimates.

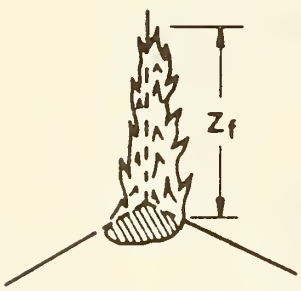

$$Z_{f\ min} = (0.075\ m/kW/^{2/5})\ \dot{Q}^{3/5} \text{ for the continuous flame} \quad (11)$$

$$Z_{f\ max} = (0.118\ m/kW^{2/5})\ \dot{Q}^{3.5} \text{ for the flame tip} \quad (12)$$

Fig. B8b. Corner Fire Scenario.

5. Radial Flame Impingement and Heat Flux to a Ceiling

Now that flame height has been estimated, it is possible to estimate radial flame impingement on a ceiling and heat flux at a ceiling using equations offered in a report by You and Faeth [12]. When the height of a free burning flame exceeds the height of the ceiling, flame impingement would occur for that fire burning in a confined geometry. That effect is shown in Figure B8 where H_R gives the radial flame impingement length.

It has been found [12] that the height (H_f) of a free burning fire in the open generally exceeds the sum of the ceiling height (H) and impingement length (H_R) under these conditions. Thus, for a given fire energy release rate $\dot{Q}$, once H_f exceeds the ceiling height, the radial flame extension can be estimated from the following formulae.

For a ceiling with no side walls,

$$\frac{H_R}{D} = 0.5\ [(H_f - H)/D]^{0.96}; \quad (13)$$

and for a ceiling with side walls,

$$\frac{H_R}{D} = 0.69\ [(H_f - H)/D]^{0.89} \tag{14}$$

where D is the fire base diameter and H_f can be found from Eq. (8). (Here Z_f and H_f are the same; since we have not attempted to unify our notation but have retained the notation of the original source.)

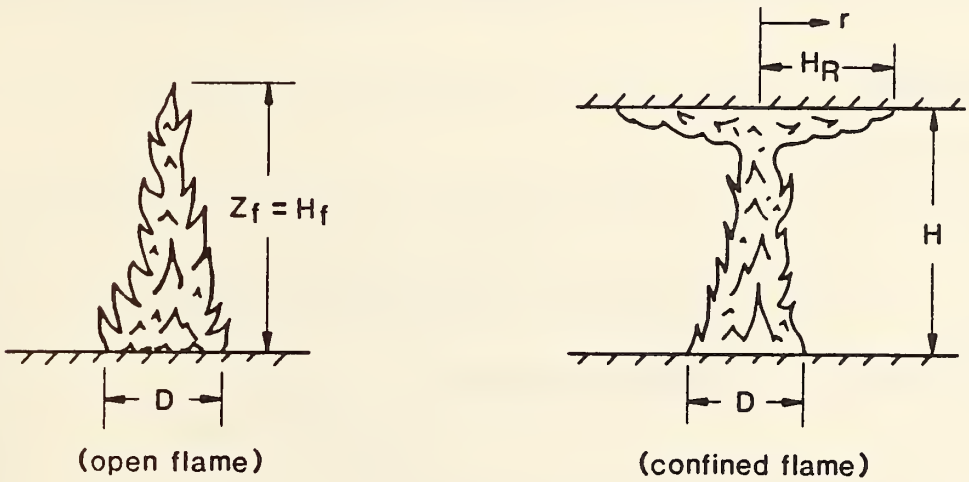

Figure B9. Flame length and geometric environment.

From the work of You and Faeth [12] an estimate of the incident (primarily convective) heat flux to the ceiling just above the fire can be found. This stagnation point heat flux $\dot{q}''$ is determined from the correlation:

$$\dot{q}''H^2/\dot{Q} = 31.2\ Pr^{-3/5}\ Ra^{-1/6} \tag{15a}$$

where H is the ceiling height and $\dot{Q}$ is the fire energy release rate. The equation was established for a Prandtl number of, Pr = 0.7, $H_f/H < 1.5$, $10^9 < Ra < 10^{14}$, and where flame radiative heat flux is small. The Rayleigh number, Ra, is defined as $(g\beta/\rho c_p \nu^3) = 7.9 \times 10^{12}\ kW^{-1}m^{-2}$.

$$\dot{q}'' = 0.28\ \dot{Q}^{5/6}H^{-7/3} \tag{15b}$$

where $\dot{Q}$ is in kW and H is in m. Much of the data correspond to low Ra, or small scale so this formula may yield perhaps low estimates on extrapolation to large scale. For $H_f/H > 1.5$, they found the stagnation point heat flux to decrease significantly from the above formula. For large flames, flame radiation should be added, and also hot layer gas and surface radiation should be included after the room becomes hot (> 300°C).

6. Smoke Filling of a Room

At this point in the calculation process, the basic fire has been characterized, and it is time to direct attention to changes in environmental conditions which result from the fire. In this section, estimates will be made on smoke filling time for a room. The "filling time", t_f, can be estimated as follows, i.e., t_f = time for the layer to reach a door soffit (see Figure B10) or a floor leak as in the case examined by Zukoski [13]. Figure B11 illustrates the dependence of ceiling layer height on time and heat input rate. For these results, heat loss from the smoke layer is neglected, and the room filling times are somewhat shorter than would be expected in a real fire. The governing equation and notation from Zukoski's analysis [13] are described below.

Smoke Filling Time

$$\frac{dy}{dt} + Q^* + \alpha (Q^*)^{1/3} y^{5/3} = 0 \qquad (16)$$

where

$$y = Z/H \qquad \text{nondimensional height of smoke layer interface} \qquad (17)$$

$$\tau = t \sqrt{g/H}\ (H^2/S) \qquad \text{nondimensional time} \qquad (18)$$

t = time

g = acceleration of gravity 9.8 m/s^2

H = room height

S = floor area of the room

$$Q^* \equiv \dot{Q} / (\rho_\infty T_\infty C_p \cdot \sqrt{gH} \cdot H^2) \qquad (19)$$

which is a nondimensional fire heat input parameter.

$\dot{Q}$ = energy release rate of the fire

ρ_∞ = density of the air in room

C_p = specific heat at constant pressure for air

α = 1/5.4, the mass entrainment coefficient

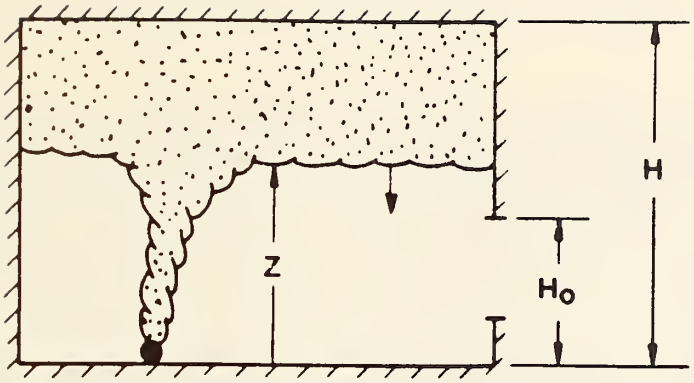

Figure B10. Room smoke filling model.

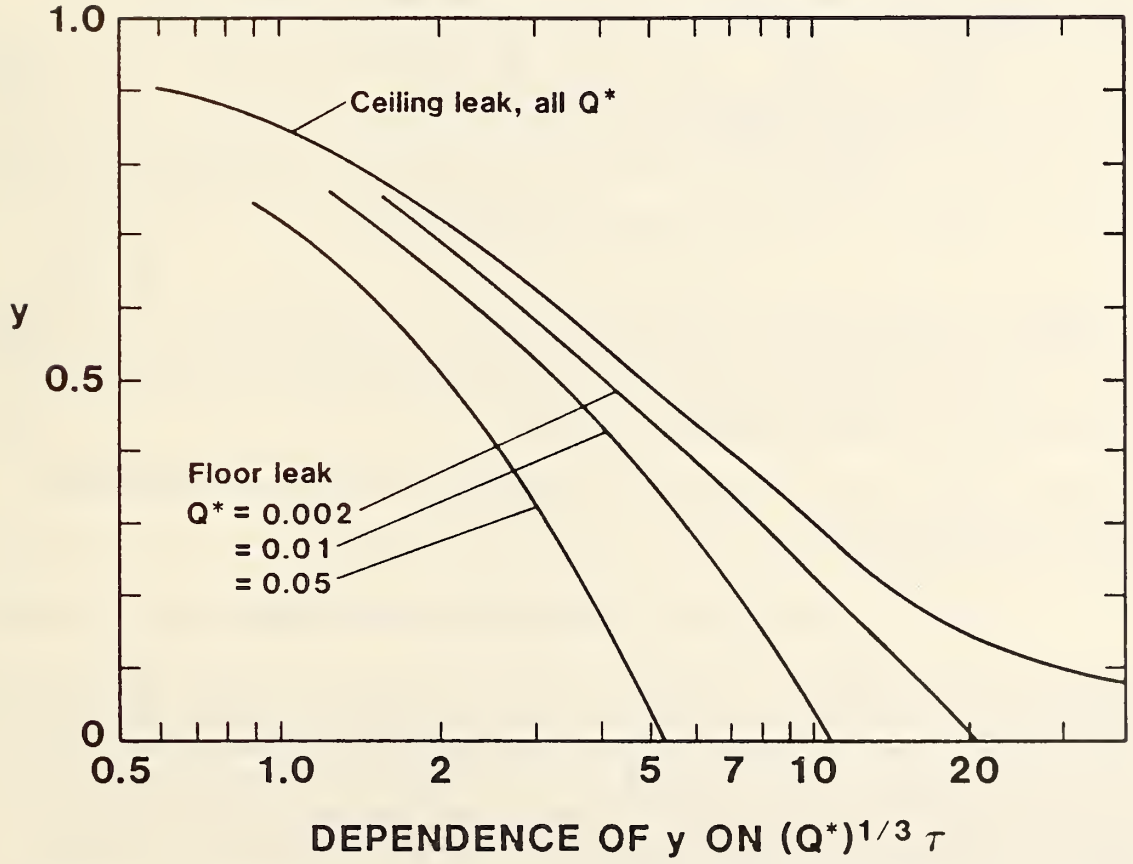

Figure B11. Ceiling layer height versus time and heat input rate [13]

In Eq. (16), if Q* is small, < 0.01

$$y \approx [1 + (\frac{2\alpha}{3})(Q^*)^{1/3}\tau]^{-3/2} \qquad (20)$$

and if Q* is large, > 0.4,

$$y \approx 1 - Q^* \tau \tag{21}$$

To solve for t_f when Q* < 0.01, Eq. (20) is solved for τ,

$$\tau \approx \frac{\left(\frac{1}{y}\right)^{2/3} - 1}{\frac{2\alpha}{3} Q^{*1/3}} \tag{22}$$

The time t_f to fill to a specific position y is then found by inverting Eq. (18) as follows:

$$t_f = \frac{\tau}{\sqrt{g/H}\,(H^2/s)} \tag{23a}$$

Smoke layer height from the floor, Z, can be calculated by Eq. (23b)

$$Z = H \left[1 + \frac{2\alpha}{3} \frac{\dot{Q}}{\rho_\infty T_\infty C_p \sqrt{gH}\, H^2} \, t \sqrt{g/H} \left(\frac{H^2}{s}\right)^{-3/2}\right] \tag{23b}$$

To solve for t_f when Q* > 0.4, Eq. (21) is solved for τ,

$$\tau \approx \frac{1 - y}{Q^*} \tag{24}$$

and then solved for t_f again using Eq. (23).

In cases where 0.01 < Q* < 0.4 one must integrate the ordinary differential Eq. (16) or use Figure B10.

7. Time to Carbon Monoxide Hazard With Smoldering Fires

The previous section presented a method for estimating smoke filling in a room when an opening is present in a wall or a leak is near the floor. This section uses smoke filling time and other data to estimate hazard time related to carbon monoxide exposure which results from a smoldering chair. Equations used in this estimate are taken from a report by Quintiere et al. [14]. In that analysis the smoke filling time is calculated using Eqs. (16) through (23) where the value of $\dot{Q}$ is estimated by

$$\dot{Q} = \dot{m}\, \Delta H \tag{25}$$

where $\dot{m}$ is the rate of mass loss due to smoldering and ΔH is the heat of reaction for the smoldering process. Here we adopt a simpler procedure based on that study to allow ease in making first order estimates.

It is shown that $\dot{m}$ could be approximated for a smoldering fire in polyurethane or cotton using

$$\dot{m} = ct \tag{26}$$

where $c = 0.206$ gm min^{-2} for polyurethane and $c = 0.33$ gm min^{-2} for cotton, and t represents time in minutes. The heat of reaction for polyurethane is $\Delta H = 15 \pm 8$ kJg^{-1} and cotton is $\Delta H = 11 \pm 1$ kJg^{-1}. These results were only for slabs of particular samples of cotton and polyurethane. Moreover the smoldering rate of an upholstered chair composed of cotton and polyurethane initially grew quadratically with time, then remained constant for the next hour. Thus, Eq. (26) with the constants given can only be taken as a rough estimate for $\dot{m}$. It was, however, found that the mass generation rate of CO could be taken as proportional to the mass loss rate in smoldering, and that constant γ was estimated as about 0.1 g CO/g fuel lost for both the polyurethane and cotton samples discussed above. Thus for those cases the CO generation rate was estimated as

$$\dot{m}_{co} = \gamma ct. \tag{27}$$

As a first estimate we will use Eq. (27) and consider a well-mixed closed volume (V) in which the smoldering takes place. The more general stratified case with "filling" was discussed in ref. [14], but in actuality the dispersal of smoldering products is not so well defined. Consequently a uniformly mixed volume is reasonable alternative. For this case the mass fraction of CO in the volume defined to be Y is given by

$$\frac{dY}{dt} = \frac{\gamma \dot{m}}{\rho V} \tag{28}$$

where ρ is the gas density. Finally adopting a critical dose of 4.5% CO-min for human incapacitation as suggested by the work of Stuart et al [14], and since the dose D can be expressed as $D = \int_0^t Y dt$ it follows from Eqs. (26-28) that

$$D = \frac{c\ \gamma\ t^3}{6\ \rho\ V}\ . \tag{29}$$

where D = 0.045 min for the critical dose, the hazard time can be estimated.

Rewriting this equation to solve for t

$$t = \left(\frac{6\ D\ \rho\ V}{c\ \gamma}\right)^{1/3} \tag{30}$$

where V = volume of the room
ρ = density of the gas
c = values shown above for polyurethane and cotton
γ = the mass fraction of CO produced per smoldering mass loss of fuel

For example, with a cotton sample $t = 25.3\ V^{1/3}$ where t is in minutes and V is m^3. The time to critical dose is finally calculated using Eq. (30).

It should be emphasized that the above analysis is very approximate and not generally applicable to all smoldering conditions. It is only offered as a first-order of magnitude estimate.

8. Temperature Rise of Hot Gases in a Compartment

A second environmental condition that requires consideration in a room fire is the resulting temperature rise. This has been studied and correlated by several different investigations. The method for estimating temperature rise, ΔT, here comes from reports by Quintiere [15] and McCaffrey, et al. [16]. This model considers temperature rise in compartments containing single or multiple wall vents, and the venting action is created only by natural convection. Figure B12 describes a compartment example and defines some parameters.

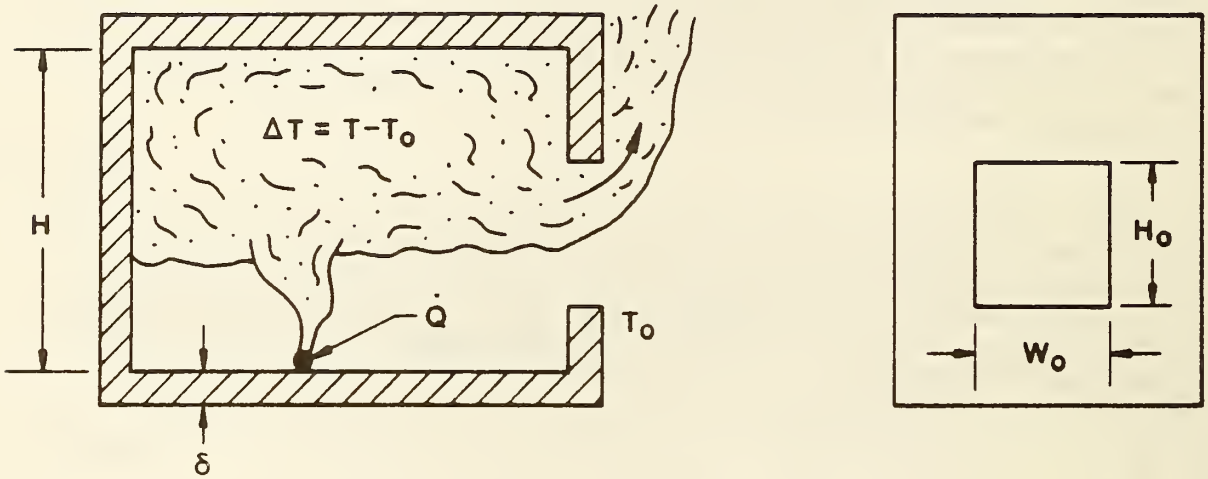

Figure B12. Compartment example.

The equation used for making this estimate of compartment gas temperature rise is

$$\frac{\Delta T}{T_o} = 1.6 \left(\frac{\dot{Q}}{\sqrt{g}\, C_p \rho_o T_o A_o \sqrt{H_o}} \right)^{2/3} \left(\frac{h_k A}{\sqrt{g}\, C_p \rho_o A_o \sqrt{H_o}} \right)^{-1/3} \tag{31}$$

where T_o = initial or ambient air temperature

$\dot{Q}$ = rate of energy release

g = acceleration of gravity 9.8 m/s^2

C_p = specific heat of air at constant pressure

ρ_o = density of ambient air

$A_o = W_o H_o$, vent area

W_o = horizontal vent dimension

H_o = vertical vent dimension

$$h_k = \begin{cases} \sqrt{k\rho c/t}, & t \leq t_p \quad \text{effective enclosure} \\ k/\delta, & t > t_p \quad \text{conductance} \end{cases}$$

k = thermal conductivity of the enclosure structure

ρ = density of the enclosure structure

c = specific heat of the enclosure structure

δ = enclosure material thickness

$t_p = \left(\frac{\rho c}{k}\right)\left(\frac{\delta}{2}\right)^2$, thermal penetration time

A = total surface area

Both $h_k A$ and $A_o\sqrt{H_o}$ should be summed for multiple structural materials and openings, respectively. The procedure for addressing multiple features is elaborated on in refrence [15].

9. Ventilation Flow Rate

Now that methods have been presented for estimating burning rates and ΔT in a fire compartment, it is time to consider ventilation flow rates in the fire. It was pointed out by Steckler, et al. [17] that the flow of air and gases in room fires has a significant influence on the development of a fire. As a fire develops, the air and gas flow rates control compartment temperature and heat transfer which then affects the rate of fire growth. When a compartment fire reaches a fully involved state, the air flow rate usually controls the fire, and the fire is then considered to be ventilation controlled. The mass flow rate of air and gases will be estimated first in this section, and ventilation limit conditions will be examined later.

In order to further understand the terminology of vent flow refer to Figure B13. Under natural convection conditions and after the hot gases fill the compartment and spill out of the vent, the flow will be countercurrent at the vent. Air will enter at a rate $\dot{m}_i$ and combustion products will flow out at a rate $\dot{m}_o$. These flows result from pressure differences (Δp) set up at the vent due to the differences in compartment and ambient gas temperatures. At the flow reversal point in the vent, the Δp is zero and this position is termed the neutral plane. The flow rates depend on the fuel mass release rate $\dot{m}_f$, the height of the neutral plane x_2, the height of the hot gas layer x_1, its temperature T, and the vent dimensions H_o and W_o. In general the vent equations are coupled nonlinear algebraic equations which we will avoid solving, but suggest the approximate procedure below.

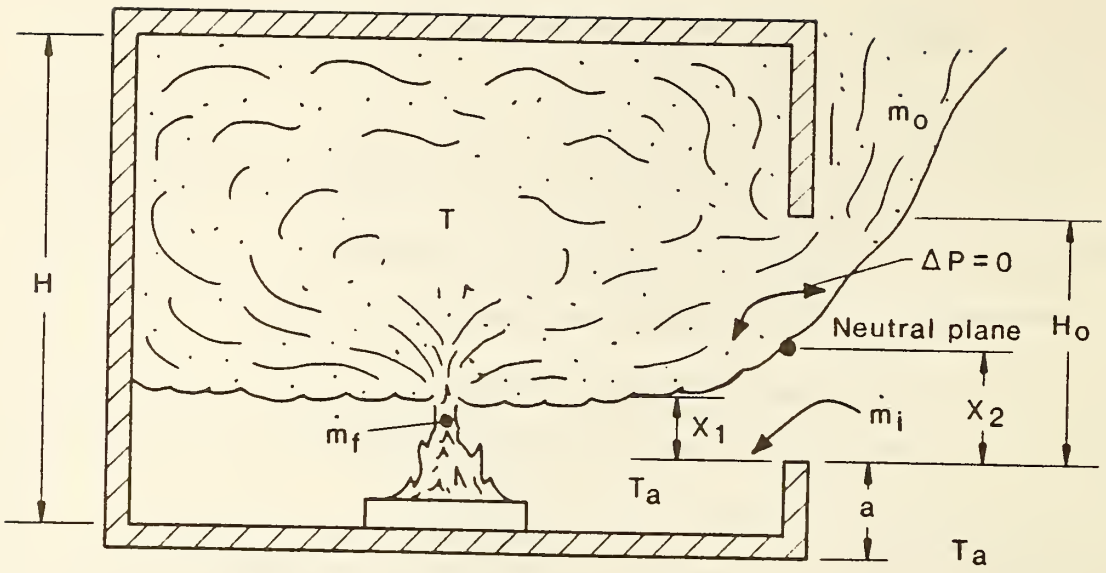

Figure B13. Sketch of compartment ventilation problem.

To make this ventilation flow rate estimate, it is necessary to assume a free burning condition. The first step in making this estimate is to calculate a fuel mass burning rate, $\dot{m}_f$, with one of the methods found in section 2, and then calculate the compartment gas temperature by the formula presented in section 8. At this point the dimensionless mass flow rate M_o can be calculated [18] using,

$$M_o = [\psi^{1/2}/(1 + \psi)]\ (1 - y_2)^{3/2} \tag{32}$$

where $$\psi \equiv \frac{T - T_a}{T_a}$$

and $y_2 = x_2/H_o$ can be estimated as 0.5 to 0.6 for $\psi \leq 1$ and for well-ventilated fires where $\dot{m}_f/\dot{m}_i$ is small as found in reference [18]. For the case of larger ψ and $\dot{m}_f/\dot{m}_i$ not small, the neutral plane can be estimated from the work of Kawagoe and Sekine [19] or from reference [18] in which $x_1 = 0$:

$$y_2 = \frac{1}{1 + \left(\frac{T}{T_a}\right)^{1/3} \left(1 + \frac{\dot{m}_f}{\dot{m}_i}\right)^{2/3}}\ . \tag{33}$$

This will yield the lower limit for y_2 when the hot layer tends to the floor and the enclosure tends toward a uniform gas temperature. Then mass flow rate out, $\dot{m}_o$, can be calculated using,

$$\dot{m}_o = \frac{2}{3} M_o C \rho_a \sqrt{2g}\ W_o\ H_o^{3/2} \tag{34}$$

where C = opening flow coefficient which is ~ 0.7

ρ_a = density of ambient gas surrounding area

g = acceleration of gravity (9.8 m/s^2)

W_o = opening width

H_o = opening height

The mass inflow rate of air, $\dot{m}_i$, can be calculated by,

$$\dot{m}_i = \dot{m}_o - \dot{m}_f \tag{35}$$

for which steady flow conditions have been assumed. Of course if $\dot{m}_f/\dot{m}_i$ is found to be large, then iteration is required in the above computations. Moreover the ratio $\dot{m}_f/\dot{m}_i$ should be compared with the mass stoichiometric fuel to air ratio to examine whether the fire is ventilation limited. We will return to this point shortly.

10. Does Flashover Occur?

The methods presented have provided a basis for predicting the fire environment up to the point of rapid transition in fire behavior. This critical point is called "flashover", and it has been defined in many different ways. A paper by Thomas, et al. [20] describes five different processes or combinations of processes that could lead to flashover. It is pointed out that flashover usually results in a sharp increase in room temperature and rate of energy release. Thomas shows that flashover is typically associated with compartment gas temperatures which range between 300-650°C. For the flashover estimates calculated in this paper it is suggested that a critical gas temperature rise of 500°C be selected. Thus for a given $\dot{Q}(t)$ the formulae for ΔT, given by Eq. (31), can be solved to find the time, t, at which ΔT = 500°C or the "flashover" time.

Alternatively, the condition for flashover with a constant energy release rate $\dot{Q}$ follows from Eq. (31) in which ΔT is set equal to 500°C. That result is given as

$$\dot{Q} = 610 \left(h_k A A_o \sqrt{H_o}\right)^{1/2} \tag{36}$$

for which $\dot{Q}$ is in kW, h_k is in $kW/(m^2K)$, H_o in m, and A and A_o are in m^2. This result says that the energy release rate to cause "flashover" depends on the compartment thermal properties, its surface area, and the vent size.

11. Mass Burning Rate in Ventilation Limited Fires

After "flashover" or in fires where small openings restrict ventilation, the fire will probably become "ventilation limited." That is the supply of air to the room is less than that amount needed for stoichiometric burning of the available gasified fuel. It can also be defined as the point when the oxygen level in the compartment reaches a low value (ideally zero) such that the reaction between fuel and oxygen ceases to produce products or proceeds very slowly.

In general, the energy release rate of the fuel burning in the compartment, is given as

$$\dot{Q} = \begin{cases} \dot{m}_f \, \Delta H \text{ for } \dot{m}_f/\dot{m}_a \leq \gamma \\ (0.233)\, \dot{m}_a \, \Delta H_{ox} \text{ for } \dot{m}_f/\dot{m}_a \geq \gamma \end{cases} \tag{37}$$

where γ is the mass stoichiometric fuel to air ratio

ΔH is the fuel heat of reaction

$\dot{m}_a$ is the air flow rate through the vent

and ΔH_{ox} is the heat of combustion per unit mass of oxygen and is taken as 13 kJ/g.

The fire is termed "fuel-controlled" for $\dot{m}_f/\dot{m}_a < \gamma$, and the energy release rate depends on the fuel pyrolysis rate. Since the air flow rate is primarily controlled by vent size, the available air supply will reach the limit for combustion as $\dot{m}_f$ increases. Thus as the fire grows, the rate of energy release within the compartment will be governed solely by the air supply rate. The excess fuel will exit the compartment with combustion continuing in the vent flame. This limit condition in which the maximum possible energy release rate is achieved in the compartment roughly occurs when $\dot{m}_f/\dot{m}_a = \gamma$ and the fire is termed "ventilation-controlled" as long as $\dot{m}_f/\dot{m}_a \geq \gamma$. Fires are generally fuel-controlled before the occurrence of flashover, and ventilation-controlled afterwards [20].

In order to estimate the point of transition to ventilation control, both the fuel mass loss rate and the air supply rate must be known. The mass loss rate $\dot{m}_f$ depends on the enclosure conditions as illustrated qualitatively below:

$$\dot{m}_f \approx \dot{m}_{fo} \left(\frac{Y_{O_2}}{0.233} + \frac{\dot{q}_e}{L} \right) \tag{38}$$

where $\dot{m}_{fo}$ - is the free burning value

Y_{O_2} - is the local oxygen concentration around the combustion region within the enclosure

$\dot{q}_e$ - is the net heat transfer rate from the enclosure to the fuel

and L - is the fuel "heat of vaporization"

There is some evidence from full-scale experiments [14] that up to flashover or shortly before, the mass loss rate in an enclosure is nearly equal to its free burn value. After flashover, the mass loss rate will differ distinctly from its free-burn value. As a first estimate to assess whether the ventilation limit has been reached, the free burn mass loss rate should be compared with the maximum vent air flow rate. The latter can be estimated by using

Eqns. (32 and 33) for $\dot{m}_f/\dot{m}_i = 0$ (i.e., small). Thus, the maximum possible vent air flow rate is for $T/T_a > 2$:

$$\dot{m}_{a,\,max} = 0.5\, W_a H_o^{3/2} \quad (kg/s) \tag{39}$$

with W_o and H_o in m. Hence the ratio of the free burn mass loss rate and maximum air supply rate can be compared with the stoichiometric ratio (γ).

After ventilation-limited conditions prevail, the mass loss rate of the fuel can not be directly computed. Nevertheless, results for wood crib fires have been empirically correlated [19,21] to yield:

$$\dot{m}_f \cong 0.09\, W_o H_o^{3/2} \quad (kg/s) \tag{40}$$

with W_o and H_o in m. An estimate of the corresponding compartment gas temperature rise might also be made by computing the energy release rate from the maximum possible air flow rate Eq. (39). The result follows [15]:

$$\Delta T = 896 \left[A_o \sqrt{H_o}/(h_k A)\right]^{1/3} \quad (^0C) \tag{41}$$

where A_o is the vent area (m^2), H_o is the vent height (m), h_k is the enclosure structure conductance (kW/m^2k) and A is the structure surface area (m^2).

12. Corridor Smoke Transfer and Filling

Much work is currently being done to develop meaningful correlations and models for smoke transfer and filling in corridors. The interest in this subject springs from the need to predict changes in environmental conditions which occur throughout a building as a fire develops. This is of great importance to life safety. An estimate made for the smoke front velocity, V_f, will be taken from work in progress by Zukoski and Kubota [22]. Figure B14 displays the phenomenon of a smoke layer progressing along a corridor.

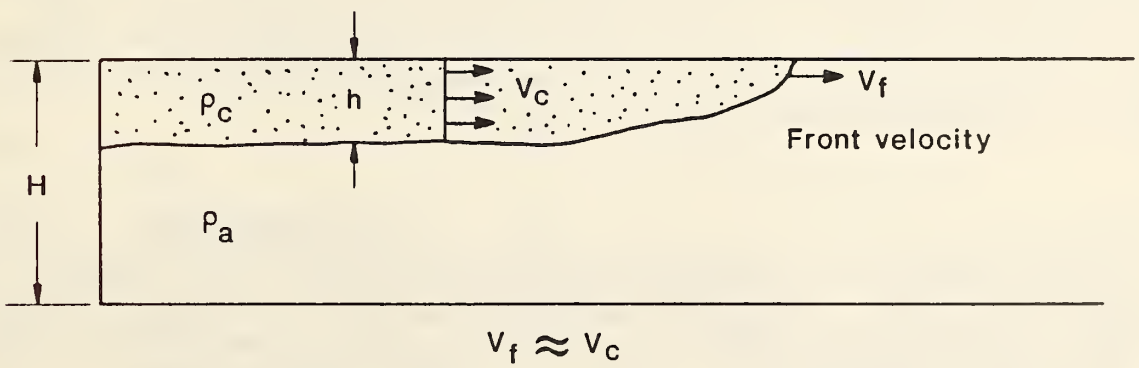

Figure B14. Corridor smoke transport.

From their preliminary analysis, we have extracted a result that represents an upper limit to the front velocity. This corresponds to the limiting case of the smoke layer filling half the corridor height and does not consider viscous effects which would retard the front speed. Thus a simple order of magnitude estimate is given below.

$$V_f \approx \tfrac{1}{2}\left[g\left(\frac{\rho_a - \rho_c}{\rho_a}\right) H\right]^{1/2} \qquad (42)$$

where g = acceleration of gravity,

ρ_a = density of ambient air,

ρ_c = density of the corridor fluid,

H = corridor height.

Density can be related to the fire room temperature provided no heat loss occurs. Thus from the ideal gas law:

$$\frac{\rho_a - \rho_c}{\rho_a} = 1 - \frac{T_a}{T}$$

where T_a = ambient temperature,

and T = gas temperature in fire room.

Subsequently the time (t_f) for velocity front movement through a corridor is estimated by

$$t_f = \frac{L}{V_f} \qquad (43)$$

where L = corridor length

Smoke filling time for a closed corridor or adjacent space to a room can be estimated using the appropriate formulas selected from section 6. But that approach would ignore the geometrical aspects of the room and corridor and their connecting doorway. It necessitates treating the corridor and room space as a single volume. Alternatively, work by Jones and Quintiere [23] suggest another approach. Figure B15 illustrates this smoke filling from a room fire to a closed adjacent space.

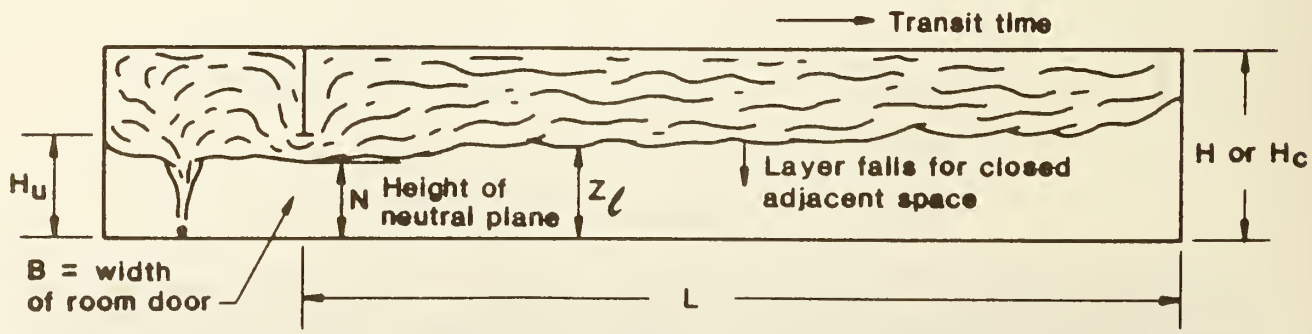

Figure B15. Smoke filling by a fire room to a closed adjacent space.

In this method a scaling parameter, $\overset{*}{P}$, for the room door is considered, where

$$\overset{*}{P} = B(H_u)^{3/2}/(H_c)^{5/2} \qquad (44)$$

where B = width of the connecting door,

H_u = height of connecting door,

H_c = height of corridor.

A correlation based on dimensionless variables was developed using both experimental and computational results. The conditions examined were a room and closed corridor of equal height (H_c = 2.32 m), a fixed room door height (H_n = 2.0 m), variable door widths ($0.13 \leq B \leq 1.07$ m), and varying heat release rates ($25 \leq \dot{Q} \leq 225$ kW). These conditions are representative of many building and developing fire conditions. The correlation is presented in Figure B16 which gives the dimensionless filling time τ as a function of the fire and door parameters, $\overset{*}{Q}$ and $\overset{*}{P}$, respectively. The time for filling was selected as the time for the smoke layer to descend to 1 m above the corridor floor. The dimensionless parameters are defined as follows:

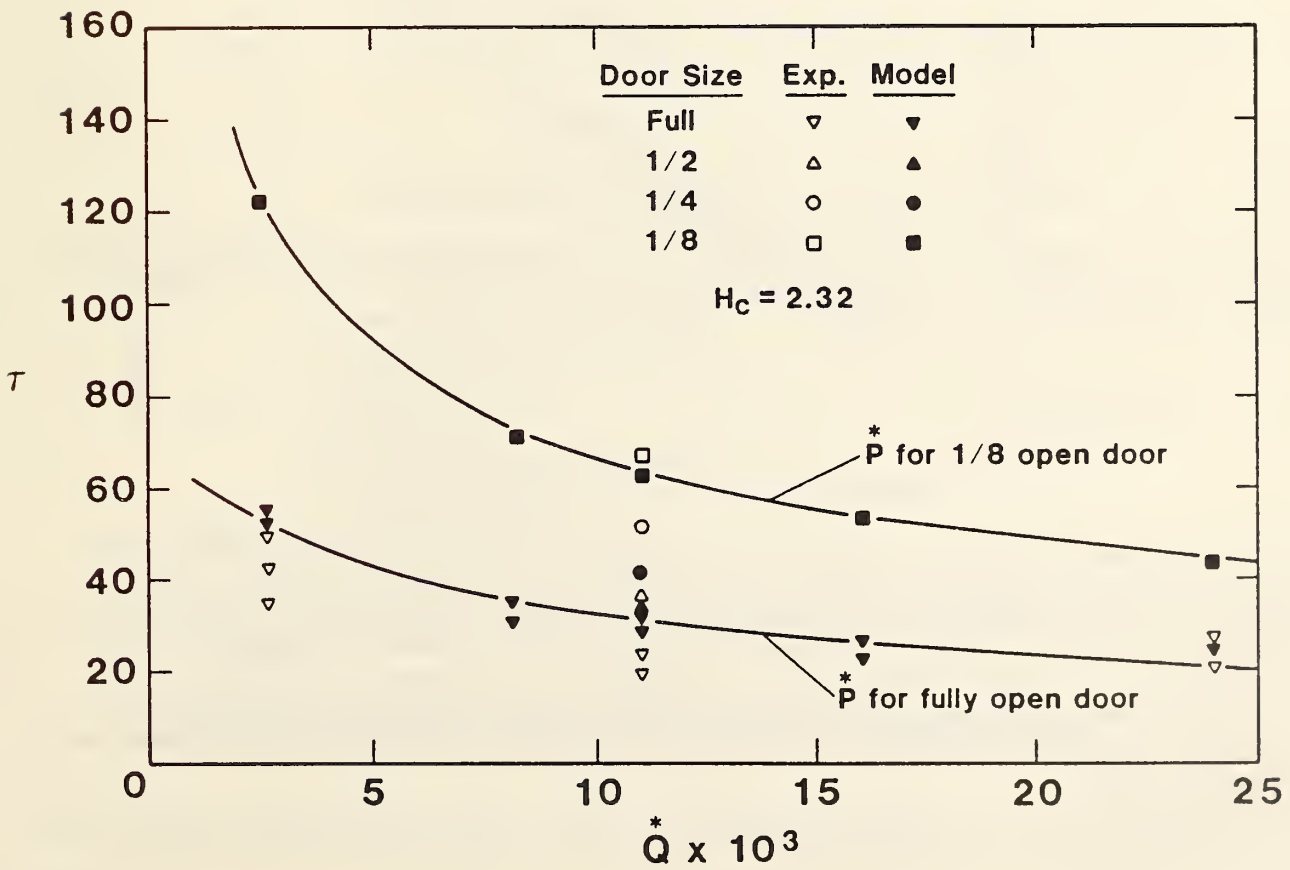

Figure B16. Dimensionless corridor smoke filling time [23]

$\overset{*}{Q}$ represents dimensionless heat release rate and is defined by the equation

$$\overset{*}{Q} = \dot{Q}/(C_p T_a \overset{*}{m}) \tag{45}$$

where $\dot{Q}$ = net heat release rate

C_p = specific heat of air

T_a = ambient temperature

and $\overset{*}{m}$ = a dimensionless characteristic mass flow which is defined as

$$\overset{*}{m} = \rho_a (gH_c)^{1/2} H_c^2 \tag{46}$$

where ρ_a = ambient density

g = acceleration of gravity

H_c = height of corridor.

The dimensionless time τ in Figure B16 is given as

$$\tau = t(\overset{*}{m}/\rho_a A H_c) \tag{47}$$

where t = time (s)
and A = floor area for the corridor or adjoining space

To make an estimate for filling time t, a $\dot{Q}$ is selected from which $\overset{*}{Q}$ is calculated. Using this $\dot{Q}$, t can be determined from Figure B16. Rearranging Eq. (47) to solve for t yields

$$t = \frac{\tau}{(\overset{*}{m}/\rho_a A H_c)} \tag{48}$$

13. Smoke Concentration and Visibility

The production of smoke in fires is an important feature in evaluating life safety. Technically smoke might be considered to include particles, hot combustion products, and toxic gases. Here we will only address the particulate nature of smoke and its effect on visibility. Smoke obscures vision by the reduction of light transmission. Smoke may also reduce vision by irritating the eyes. In this section estimates for smoke concentration and visibility will be calculted for a closed system which consists of a room and adjacent space.

The production rate of smoke particles $(\dot{m}_s)$ in a fire can be expressed as

$$\dot{m}_s = \chi_s \dot{m}_f \tag{49}$$

where χ_s = fraction of particulate mass to fuel mass loss

$\dot{m}_f$ = fuel mass loss rate

The objective is to compute this production rate and relate it to visibility. Some background on needed data and applications can be found in reports by Quintiere [24], Babrauskas [25] and Tewarson [26]. An approximate relationship to predict visibility, defined to be L_v the length one can see through smoke when no eye irritation is present, is given as

$$L_v = k_v/(D/L) \tag{50}$$

where D/L is the optical density per unit path length
k_v is a constant selected from Figure B17.

This relationship is derived from the results shown in Figure B17 [24] and is merely an approximate fit to those data. Of course the selected value for k_v should be consistent with those results but could also represent a conservative design value. To apply Eq. (50) to a particular situation we must compute (D/L) for that fuel and the configuration it burned in.

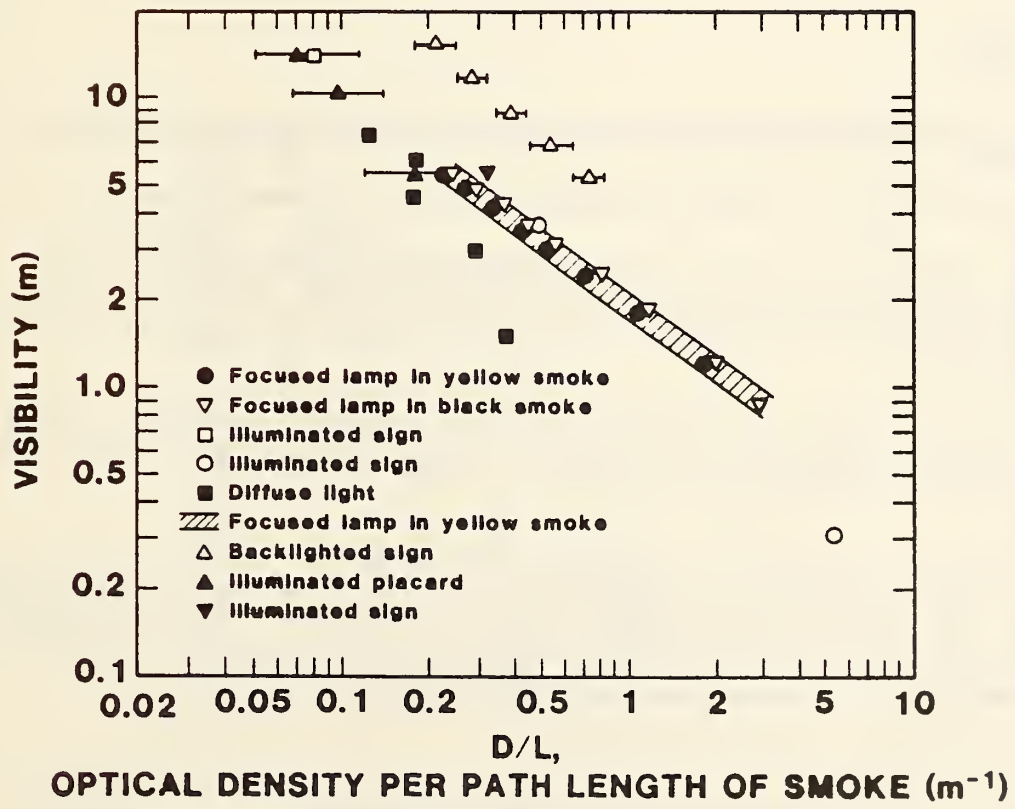

Figure B17. Visibility results derived from Rasbash [27], Jin [28] and Lopez [29].

To compute (D/L) for a closed system, for example a room and adjacent space, the following relationship must be integrated over time:

$$\frac{d(D/L)}{dt} = \frac{\alpha \chi_s}{V} \dot{m}_f \tag{51}$$

where t is time
α is the particle optical density
and V is the volume of the enclosed space.

The mass loss rate $\dot{m}_f$ should be initially estimated from free burn analysis as before. This will be valid in the early stages of the fire. Data on α and χ_s, properties of the burning fuel, are needed for each fuel. Seader and Ou [30] suggest $\alpha \approx 3300$ m^2/kg for fuels burning in air, and these results for a wide range of fuels are given by Tewarson [26]. (However Tewarson defines x_s and Y_s and reports σ, which is related to α, as $\alpha = \sigma/(2.303\ Y_s)$.) Also αx_s can be estimated from the Smoke Density Chamber Test Method described in ASTM E-662. It can be shown that

$$\alpha \chi_s = \frac{D_{s,max}}{m''} \tag{52}$$

where $D_{s,max}$ is the maximum specific optical density measured in ASTM E-662

and m" is the mass of sample consumed per unit of exposed surface area.

Of course the values of α and χ_s for a given material will depend on the exposure conditions during the burning of those samples. For first order estimates these effects are ignored, but judgment must be used in the application of such data.

The estimate based on Eq. (51) assumes that the volume of interest is well mixed and here the filling time has been ignored. Table B3 gives some representative values for α and χ_s.

An important point that should be noted in the discussion above is that in ventilation limited conditions, $\dot{m}_f$ depends on air flow and χ_s has been shown to increase. The ventilation parameter $A_o\sqrt{H_o}$ is reduced. This is shown in Figure B18 from the work of Saito [31] for plywood burning in an enclosure of floor area A.

Table B3

Smoke properties for selected materials burning in air [26]

Material	Particle Optical Density α ($10^3 m^2/kg$)	Fraction of Particulate Mass to Fuel Mass Loss χ_s (-)
Oak	3.17	0.013
PMMA	4.65	0.021
Polyurethane foam flexible (GM-25)	0.426	0.32
Granular Polystyrene	2.11	0.15

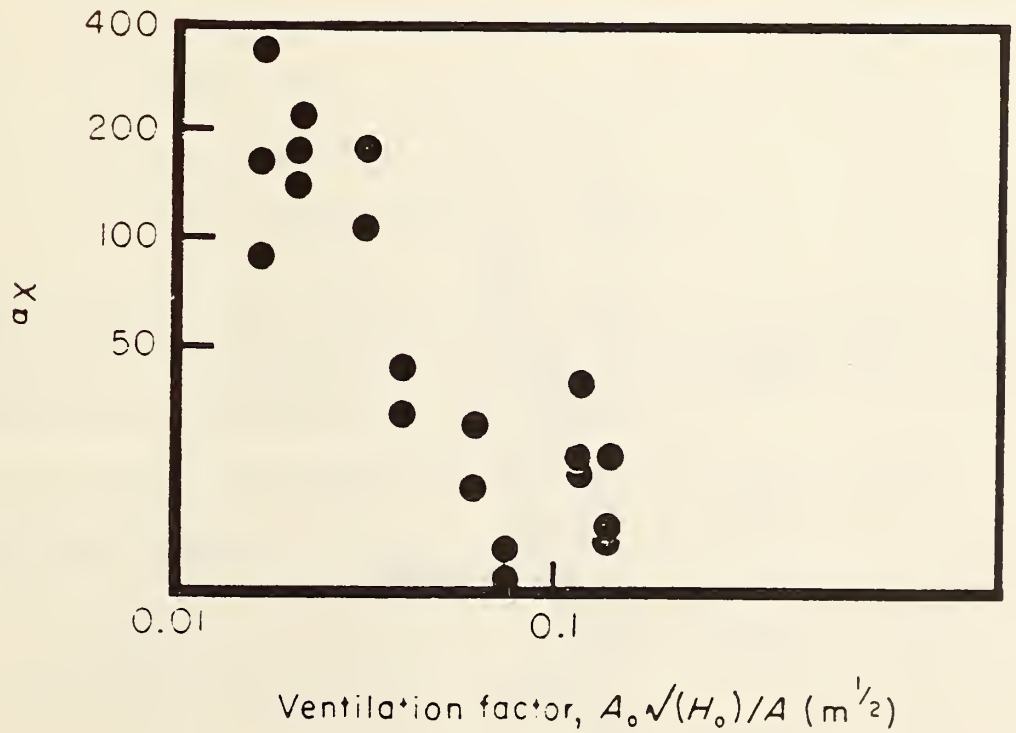

Figure B18. Smoke production for plywood as a function of ventilation factor from Saito [31]

14. Estimation of Flame Spread Rates

After an unwanted fire has started flames spread away from the point of origin. The rate of flame spread, V_f, is affected by several environmental factors and the thermophysical/thermochemical properties of the materials. For solids of thickness > 1 mm Eq. (53) Quintiere and Harkleroad [32] illustrate some of these variables.

Solids

$$V_f \propto \frac{(T_f - T_{ig})^2}{k\rho c(T_{ig} - T_s)^2} \tag{53}$$

where T_f - is the flame temperature which depends on available oxygen

T_{ig} - is the ignition temperature

T_s - is the upstream surface temperature resulting from an external heat flux.

Figure B19 schematically depicts the plume spread phenomena.

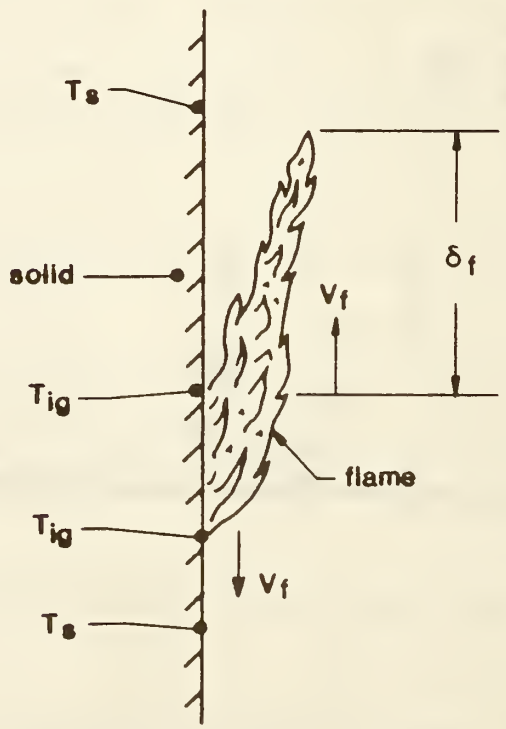

Figure B19. Sketch of flame spread model.

The relationship shown above can be converted into an estimate of downward flame spread rate using,

Flame Spread Opposed to Flow (downward)

$$V_f \approx \frac{\Phi}{k\rho c(T_{ig} - T_s)^2} \tag{54}$$

where

$$\Phi = V_a\,(k\rho c)_g\,(T_f - T_{ig})^2 \tag{55}$$

and

$$V_a = \frac{\left(\frac{k}{\rho c}\right)_g\, g\,(T_f - T_\infty)}{T_\infty}^{1/3} \qquad \text{opposed flow characteristic gas velocity under natural convection conditions} \tag{56}$$

where k_g = thermal conductivity of gas phase

ρ_g = specific heat of gas

c_g = specific heat of gas

g = gravitational acceleration (9.8 m/s^2)

T_f = adiabatic flame temperature

T_∞ = ambient and initial temperature

It has been found for a wide range of materials that Φ generally ranges between 1 and 15 $(kW)^2/m^3$; T_{ig}, ranges between 250 and 600°C; and $k\rho c$ ranges between 0.01 and 1.0 $(kW/m^2K)^2s$ [32]. These are to be considered pseudo-properties valid for Eq. (54) under opposed flow natural convection flame spread in vertical orientation.

For upward flame travel, flame spread rate can be described by:

Upward Flame Spread

$$V_f \approx \frac{(\dot{q}''_f)^2\,\delta_f}{k\rho c\,(T_{ig} - T_s)^2} \tag{57}$$

where $\dot{q}''_f$ = heat transfer per unit time and per unit area

and δ_f = flame extension length

Practical applications of Eq. (57) have not been developed, and general methods for predicting $\dot{q}''_f$ and δ_f do not exist.

15. Flame Spread Over Liquids

Glassman [33] reports on recent research efforts and theories for flame spread over liquids. As is shown in Figure B20, there are basically two different regimes for fires on liquids. One regime relates to flame spread which is controlled by gas phase phenomena when the bulk liquid temperature (T_L) reaches its flash point or, for sustained burning, its fire point temperature T_f. The other regime occurs when the bulk liquid temperature is below its fire point temperature. This slower flame spread phenomena depends on the evaporation of the liquid to sustain and control the process. As the liquid temperature rises above the fire point temperature to T_{LSt}, a stoichiometric fuel-air mixture is formed near the surface, and consequently flame spread occurs in the gas phase. This rate of flame spread is related to the bulk liquid temperature and its surface tension.

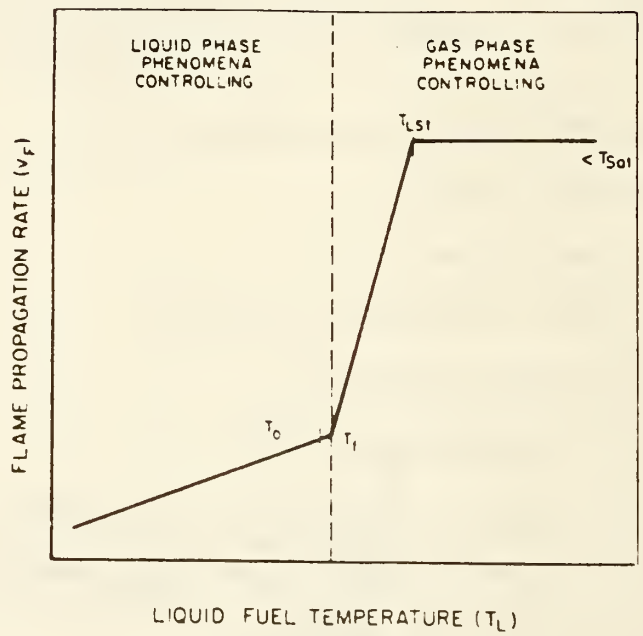

Figure B20. Schematic of the flame spreading rate as a function of the liquid temperature of the fuel [33].

A report by Williams [34] gives a qualitative formula for the flame spread rate, V_f, on liquid fuels.

$$V_f = \frac{\sigma'}{\mu_\ell} \left(\frac{\mu_\ell^2 \, \ell}{\rho_\ell \sigma'} \right)^{1/3} \tag{58}$$

where σ' = gradiant in surface tension

$$\sigma' = \frac{d\sigma}{dT} \left(T_{ig} - T_o \right) / \ell \tag{59}$$

T_{ig} = liquid ignition temperature

T_o = initial liquid temperature

ℓ = length characteristic forward flame heat transfer to the liquid

μ_ℓ = liquid viscosity

ρ_ℓ = liquid density

The application of this equation to practical problem solving is not straightforward since ℓ depends on the heat transfer characteristics of the particular problem. Referral to references [33,34] will give some further background and insight on potential applications.

16. Fully Developed Fire Burn Time

Once a fire has started and has become fully developed, it is of interest to be able to estimate the duration of burning. This can be easily estimated by

$$t_b \approx \frac{m_f}{\dot{m}_f} \tag{60}$$

or

$$m_f = \int_o^{t_b} \dot{m}_f \, dt \tag{61}$$

where m_f is the mass of fuel available to burn (vaporize) and $\dot{m}_f$ is the burning (vaporization) rate of the fuel under the specified environmental conditions. The value for $\dot{m}_f$ can be estimated using the equations located in section 2.

17. Conclusion

To conclude this paper, it would be appropriate to use the techniques presented to make estimates for the development of a hypothetical fire. An exercise of this type is presented in the "Example" which follows section 18.

This report has brought together a number of techniques developed by various researchers for evaluating the fire environment. These predictive methods can be useful in estimating many of the critical elements related to fire behavior and help provide a better understanding of this complex phenomenon. It should be remembered when using this report while making predictions that the results are only estimates. These estimates, which spring from the state-of-the-art, are meant to provide a reasonable approximation and in some cases just an order of magnitude for the particular elements under study. More accurate predictions typically involve more complex calculations using more powerful methods than a simple calculation. In many cases, additional research is needed to formulate new solutions, derive more data, and to develop more sophisticated fire models than currently exist. Nevertheless the approach presented here provides, in addition to its estimates, a conceptual framework for what we can do and what we must learn to do.

18. References

1. Delichatsios, M.A., Fire Growth Rates in Wood Cribs, Combustion and Flame, 27, 267-278 (1976).

2. Heskestad, G., Modeling of Enclosure Fires, 14th Symposium (International) on Combustion, The Combustion Institute, Pittsburgh, p. 1021, (1973).

3. Lawson, J.R., Walton, W.D., Twilley, W.H., Fire Performance of Furnishings as Measured in the NBS Furniture Calorimeter. Part I, National Bureau of Standards (U.S.) NBSIR 83-2787 (1983).

4. Babrauskas, V., Combustion of Mattresses Exposed to Flaming Ignition Sources - Part I. Full Scale Tests and Hazard Analysis, National Bureau of Standards, (U.S.), NBSIR 77-1290, (1977).

5. Orloff, L., Fire Growth on Polyurethane Foam, Modak, A.T., ed., Influence of Enclosures on Fire Growth, Volume II - Analysis, Tech. Report, FMRC J.I. OAOR3.BU, RC78-BT-24, Factory Mutual Research Corp., Norwood, MA (July 1978).

6. Modak, A.T., Croce, P.A., Plastic Pool Fires, Combustion and Flame, 30, 251-265, (1977).

7. Burgess, D.S., Grumer, J., Wolfhard, H.G., Burning Rates of Liquid Fuels in Large and Small Open Trays, International Symposium on the Use of Models in Fire Research, Publication 786 National Academy of Sciences, (November 1959).

8. Modak, A.T., Thermal Radiation from Pool Fires, Combustion and Flame, 29, 177-192 (1977).

9. McCaffrey, B.J., Purely Buoyant Diffusion Flames: Some Experimental Results, National Bureau of Standards, (U.S.) NBSIR 79-1910 (1979).

10. Zukoski, E. E., Kubota, T., Cetegen, B., Entrainment in Fire Plumes, Fire Safety Journal, 3, 107-121 (1980/81).

11. Hasemi, Y., Tokunaga, T., Modeling of Turbulent Diffusion Flames and Fire Plumes for the Analysis of Fire Growth, Fire Dynamics and Heat Transfer, The American Society of Mechanical Engineers, 21st National Heat Transfer Conference, HTD-Vol. 25, (1983).

12. You, H.Z., Faeth, G.M., Ceiling Heat Transfer During Fire Plume and Flame Impingement, Fire and Materials, Vol 3, (1979).

13. Zukoski, E.E., Development of a Stratified Ceiling Layer in the Early Stages of a Closed-Room Fire, Fire and Materials, Vol. 2, No. 2, (1978).

14. Quintiere, J.G., Birky, M., McDonald, F., Smith, G., An Analysis of Smoldering Fires in Closed Compartments and Their Hazard Due to Carbon Monoxide, Fire and Materials, Vol. 6, Nos. 3 and 4, (1982).

15. Quintiere, J.G., A Simple Correlation for Predicting Temperature in a Room Fire, National Bureau of Standards (U.S.), NBSIR 83-2712, (1983).

16. McCaffrey, B.J., Quintiere, J.G., Harkelroad, M.F., Estimating Room Temperatures and the Likelihood of Flashover Using Fire Test Data Correlations, Fire Technology, 17, 2, p. 98, (May 1981).

17. Steckler, K.D., Quintiere, J.G., Rinkinen, W.J., Flow Induced by Fire in a Compartment, Nineteenth Symposium (International) on Combustion, The Combustion Institute, pp. 913-920, (1982).

18. Quintiere, J.G., Steckler, K., Corley, D., An Assessment of Fire Induced Flows in Compartments, Fire Science and Technology, Vol. 4, No. 1, p. 1-14, (June 1984).

19. Kawagoe, K., Sekine, T., Estimation of Fire Temperature - Time Curve for Rooms, Ministry of Construction, Japanese Government, (June 1963).

20. Thomas, P.H., Bullen, M.L., Quintiere, J.G. and McCaffrey, B.J., Flashover and Instabilities in Fire Behavior, Combustion and Flame, 38, 159-171, (1980).

21. Thomas, P.H., Heselden, A.J.M., Law, M., Fully-Developed Compartment Fires -- Two Kinds of Behavior, Ministry of Technology and Fire Offices Committee, Fire Research Station, Borehamwood, England Technical Paper No. 18, (1967).

22. Zukoski, E.E., Kubota, T., Experimental Study of Environment and Heat Transfer In a Room Fire, Final Report, Grant NB82NADA3033, National Bureau of Standards, (U.S.), (July 1984).

23. Jones, W.W., Quintiere, J.G., Prediction of Corridor Smoke Filling by Zone Models, Combustion Science and Technology, Vol. 35, pp. 239-253, (1984).

24. Quintiere, J.G., Smoke Measurements: An Assessment of Correlations Between Laboratory and Full-Scale Experiments, Fire and Materials, Vol. 6, Nos. 3 and 4, (1982).

25. Babrauskas, V., Applications of Predictive Smoke Measurements, Journal of Fire and Flammability, Vol. 12, p. 51, (January 1981).

26. Tewarson, A., Physico-Chemical and Combustion/Pyrolysis Properties of Polymeric Materials, National Bureau of Standards (U.S.), NBS-GCR-80-295, (1980).

27. Rasbash, D.J., Smoke and Toxic Products Produced at Fires, Plastics Institute Transaction and Journal, pp. 55-61, (January 1967).

28. Jin, T., Visibility through Fire Smoke (Part 2), Report of the Fire Research Institute of Japan, Nos. 33, 31, (1971).

29. Lopez, E.L., Smoke Emission from Burning Cabin Materials and the Effect on Visibility in Wide-Bodied Jet Transports, Journal of Fire and Flammability, Vol. 6, (October 1975).

30. Seader, J.D., Ou, S.S., Correlation of the Smoking Tendency of Materials, Fire Research, 1, 3-9, (1977).

31. Saito, F., Smoke Generation from Building Materials, 15th Symposium (International) on Combustion, The Combustion Institute, 269 (1974).

32. Quintiere, J.G., Harkelroad, M., New Concepts for Measuring Flame Spread Properties, presented at Symposium on Application of Fire Science to Fire Engineering, ASTM, SFPE, (June 1984).

33. Glassman, I., Dryer, F.L., Flame Spreading Across Liquid Fuels, Fire Safety Journal, Vol. 3, Nos. 2-4, (January-March 1981).

34. Williams, F.A., Mechanisms of Fire Spread, Sixteenth Symposium (International) on Combustion, The Combustion Institute, 1281-1294, (1976).

19. EXAMPLE

This exercise is designed to provide an example of the use of the predictive methods presented in this report. It is intended as a hypothetical illustration and should not be construed as representative of the hazard associated with the particular items, materials and occupancy configuration selected. The first step in analyzing a fire scenario is to define the problem in terms of information required by the relevant predictive formulae.

Problem:

The fire takes place in a hotel room. A fire starts from a cigarette lighter in the center of a bed with a polyurethane foam mattress. The room door is left 1/4 open as the occupant flees the room. Figure B21 shows the plan for the hotel section being studied.

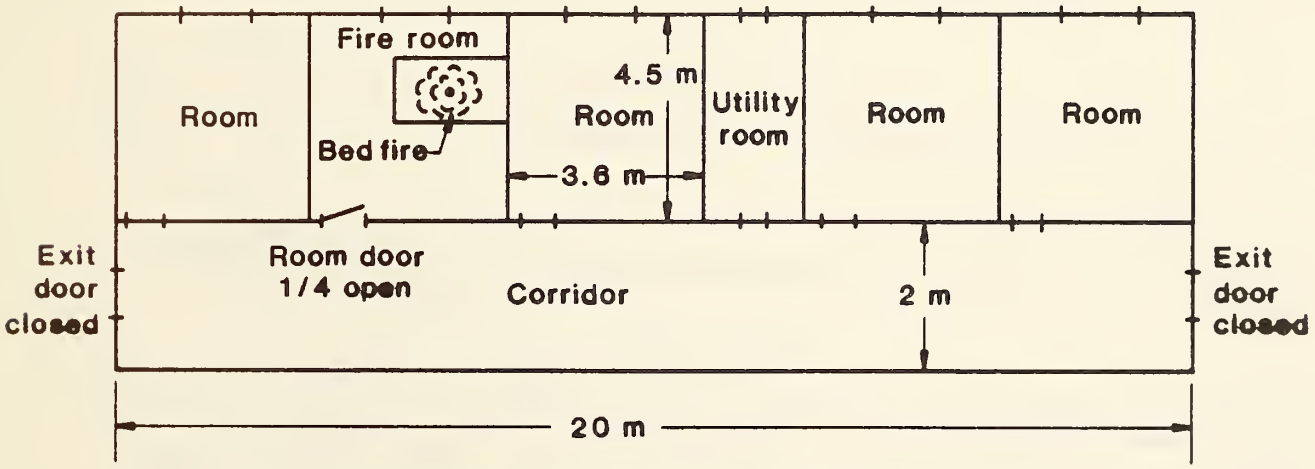

Note: Ceiling height in rooms and corridors 2.4 m.
All doors are closed except the fire door.

Figure E1. Room Fire Example

Analysis of Fire Growth and Consequences

In this section, the prediction methods presented earlier are used to calculate mass loss rate, heat release rate, flame height, ceiling heat flux, temperature rise, ventilation flow rate, visibility, smoke filling, and smoke transport for the sample problem. The data required to make these calculations are provided as well as the assumptions used to simplify the calculation process. Tables of predicted values are presented and selected results are shown graphically.

Mass Loss Rate

The first step in these predictions of fire growth and hazardous conditions is the determination of an expression for energy generation rate of the fire. Using Eq. (3) with $\beta = 0$ yields the following expression for fuel mass loss rate.

$$\dot{m} = \alpha e^{\alpha t} \text{ where } \alpha = 0.03$$

The solution to this expression is shown in Table E1 and Figure E2 for times up to 250 s. Mass loss rates for times from 250 s to 300 s are calculated using the steady state burning formula for wood cribs:

$$\dot{m}_f = 0.09\, W_o H_o^{3/2}$$

where $W_o = 0.23$

$H_o = 2$

This represents the ventilation-limited fire case. It is employed at the time when the ratio of fuel mass loss rate to air flow rate to the room exceeds its stoichiometric ratio (8).

Heat Release Rate

Heat release rate was calculated using the equation:

$$\dot{Q} = \dot{m}\Delta H$$

where $\Delta H = 15.7$ (kJ/g) for the polyurethane foam mattress in the example.

Radiant Flux

From the heat release rate the radiant heat transfer to a nearby surface can be calculated using Eq. (7). In this prediction, it is assumed that R_o, the distance from the heat source to the wall is 1.8 m. The χ_r value for polyurethane foam in this example is 0.35. Both values for $\dot{Q}$ and $\dot{q}''_o$ (R_o) are presented in Table E1 The radiant flux $\dot{q}''_o$ (R_o) as a function of time is shown in Figure E3.

Flame Height

The values for flame height, H_f, and ceiling flame impingement length, H_R, in Table E1 and Figure E4 were calculated using Eqs. (8) and (14), respectively. In Eq. (14), the value for H = 1.8 m since the bed height is subtracted from the overall ceiling height, and D was selected as a constant of 0.5 m. (Although the fire is growing, it is not strongly dependent on D.)

Ceiling Heat Flux

Table E1 and Figure E3 also contain predictions for heat flux to the room's ceiling. These results were developed using Eq. (15b). The values for radiant flux derived from Eq. (7) were added to values from Eq. (15b) to predict the total heat flux to the ceiling. In this example radiation from the hot gas layer has not been included in the total heat flux to the ceiling. However, an upper limit for radiation to the ceiling from the hot gas layer can be estimated as σT^4 where σ is 5.6697×10^{-8} W/m^2 - K^4.

Temperature Rise

Predictions for gas temperature rise, ΔT, in the room are presented in column 8 of Table E1. Also see Figure E5. These values were generated using Eq. (31), but before the various temperatures were calculated thermal penetration times, t_p, for the gypsum walls and plywood floors were determined. The following parameters were used in these calculations:

Gypsum wallboard (walls/ceiling)

$t_p = 393$ s

$\rho = 960$ kg/m^3

$c = 1.1$ kJ/(kg-K)

$k = 1.7 \times 10^{-4}$ kJ/(m-K)

$\delta = 0.0159$ m

Plywood (floor)

$t_p = 711$ s

$\rho = 540$ kg/m^3

$c = 2.5$ kJ/(kg-K)

$k = 1.2 \times 10^{-4}$ kJ/(m-K)

$\delta = 0.0159$ m

As a result of these calculations, it was found that values for h_k in Eq. (31) would be determined using $\sqrt{k\rho c/t}$ where $t \leq t_p$. At this point, it is important to note that new values for h_k are calculated with each new time in the prediction of ΔT. For $t \leq t_p$, h_k was calculated by

$$h_k = \frac{A_1 h_{k,1} + A_2 h_{k,2}}{A}$$

where

$A_1 = 55.08$ m^2 area for walls and ceilings

$A_2 = 16.2$ m^2 area for floor

$A = 71.28$ m^2 total

and $h_{k,1}$ and $h_{k,2}$ correspond to the gypsum board and plywood respectively.

When extended calculations are made for $t > t_p$ for either the walls and ceiling or floor, k/δ should be substituted into the above equation. For

ΔT calculations at times greater than the point of flashover, Eq.(41) was used. Values for the parameter in Eq. (31 and 41) are as follows:

$g = 9.8\ m/s^2$

$c_p = 1.046\ kJ/(kg\text{-}K)$

$\rho_o = 1.25\ kg/m^3$

$T_o = 293\ K$

$A_o = 0.46\ m^2$

$H_o = 2\ m$

Ventilation Flow Rate

Since both $\dot{Q}$ and ΔT are now available, ventilation flow rate is calculated. In this procedure, Eqs. (32, 33, 34 and 35) are used to make the predictions. For times down to 220 s where $\psi \leq 1$, $y_2 = 0.5$ was used in the calculation. For $\psi > 1$, Eq. (33) was used to calculate an estimated value of y_2. This was done by substituting the preceeding result of $\dot{m}_i$ into the equation. The values of M_o and $\dot{m}_o$ were determined using Eqs. (32 and 34), and $\dot{m}_i$ results were found with Eq. (35). The values used in this calculation were as follows:

$\rho_a = 1.25\ kg/m^3$

$g = 9.8\ m/s^2$

$W_o = 0.23\ m$

$H_o = 2\ m$

It can be seen in Table E1 and Figure E6 that the ventilation starts to drop off at about 220 s and then starts to rise again. The 220 s point is where the estimated value for y_2 was started, and it is continued until the ventilation limit condition is reached at a time between 250 and 255 s. At this point and beyond, the $\dot{m}_f$ value is based on steady state enclosure ventilation limited formula, and the calculation for $\dot{m}_i$ was stopped.

Corridor Visibility

The last column in Table E1 consists of predictions of visibility, L_v, in the corridor. Also see Figure E7. The equation used in this prediction was as follows:

$$L_v = \frac{k_v V}{\alpha x} \int_o^t \dot{m}\, dt$$

where

$k_v = 2$

V = (Width)(length)(height) of corridor
(2m) (20m) (2.4m)

and

$$\int_o^t \dot{m}\, dt = \int_o^t \alpha e^{\alpha t} dt = e^{\alpha t} - 1 \Big|_o^t \text{ for mattress}$$

$\alpha = 3300\ m^2/kg$

$\times = 0.3$ g smoke particulates/g fuel

These predictions show that visibility would be about 0.1 m when flashover (based on $\Delta T = 500°C$) occurs. (It should be noted that this calculation assumes a well-mixed gas state in the corridor. But this does not occur until 181s approximately. So use of the formulae before this time will over estimate the visibility by the ratio of corridor volume to actual smoke layer volume.

Smoke Filling

Two other tables are presented in this example. Table E2 is a listing of various room smoke filling times based on different steady state heat release rates. Equation (23b) was usd to calculate these values. The following values were used in these calculations:

$\alpha = 1/5.4$

$\rho_\infty = 1.25\ kg/m^3$

$T_\infty = 293\ K$

$c_p = 1.046\ kJ/kg\text{-}k$

$g = 9.8\ m/s^2$

$H = 2.4\ m$

$s = 16.2\ m^2$

These results suggest that combustion products begin to leave the room i.e., the layer is just below the door soffit (H = 1.99 m) at about 10 to 35 s.

Table E3 contains additional predictions which provides an order of events for the fire growth example. Smoke filling time for the room was taken from Table E2, and visibility in the corridor was taken from Table E1. The value for smoke filling time in the corridor was generated using Eqs. (45, 46, and 48). Parameter values used in this calculation were as follows:

$\rho_a = 1.24\ kg/m^3$

$g = 9.8\ m/s^2$

$H_c = 2.32\ m$

$\dot{Q} = 100\ kW$

$L_c = 1.046\ kJ/kg\text{-}K$

$T_a = 293\ K$

$\tau = 47$

$A = 40\ m^2$

The time for the occurrence of flashover and the ventilation limit time was taken from Table E1. The time for flashover is based on a 500°C temperature rise, and the ventilation limit is based on the effective fuel-air mass ratio where

$$\gamma = \frac{\Delta H_{air}}{\Delta H_{fuel}} = \frac{3.03\ kJ/g\ air}{15.7\ kJ/g\ fuel} = 0.193\ g\ fuel/g\ air$$

This mass ratio was compared with fuel and air values contained in Table E1.

Smoke Transport

The predictions at the bottom of Table E3 were developed using Eq. (42) where

ρ_c was selected to correspond to the room temperature (T) so that

$$\frac{\rho_a - \rho_c}{\rho_a} = 1 - \frac{T_a}{T}.$$

Parameters used in this calculation were as follows:

$g = 9.8\ m/s^2$

$T_a = 293\ K$

$T = 303\ K$

$H = 2.4\ m$

Smoke transport times to the corridor ends were calculated using Eq. (43). Center line distances from the hotel room door were 4.2 m and 15.8 m respectively for the near and far ends of the corridor.

Thus a chronology of significant events and the magnitude of physical fire effects have been estimated for this scenario. It's accuracy is at least good to an order of magnitude and more exact assessments of accuracy must be based on the assumptions and support literature for each of the formulas used.

Table E1. Fire Growth Predictions

t (s)	$\dot{m}_f$ (g/s)	$\dot{Q}$ (kW)	$\dot{q}''_o$ (R_o) (kW/m^2)	H_f (m)	H_R (m)	$\dot{q}''$ (0) (kW/m^2)	ΔT (°C)	$\dot{m}_i$ (kg/s)	Corridor L_v (m)
0	0.00	0.0	-	-	-	-	-	-	-
10	0.04	0.6	-	-	-	-	-	-	-
20	0.05	0.8	-	-	-	-	-	-	-
30	0.07	1.1	-	-	-	-	-	-	-
40	0.10	1.6	-	0.28	-	0.11	1	0.034	83.6
45	0.12	1.9	-	0.29	-	0.12	7	0.090	67.9
50	0.13	2.0	-	0.30	-	0.13	8	0.095	55.7
55	0.16	2.5	-	0.33	-	0.15	9	0.101	46.1
60	0.18	2.8	-	0.35	-	0.17	10	0.106	38.4
65	0.21	3.3	-	0.37	-	0.19	11	0.111	32.1
70	0.24	3.8	-	0.39	-	0.22	12	0.115	27.1
75	0.28	4.4	-	0.42	-	0.24	14	0.124	22.8
80	0.33	5.2	-	0.44	-	0.28	15	0.128	19.3
85	0.38	6.0	-	0.47	-	0.32	17	0.135	16.4
90	0.45	7.1	-	0.50	-	0.36	19	0.142	14.0
95	0.52	8.2	-	0.53	-	0.41	21	0.149	11.9
100	0.60	9.4	-	0.56	-	0.46	24	0.157	10.2
105	0.70	11.0	0.09	0.60	-	0.52	27	0.164	8.7
110	0.81	12.7	0.11	0.64	-	0.59	29	0.169	7.4
115	0.94	14.8	0.13	0.68	-	0.67	33	0.178	6.4
120	1.10	17.3	0.15	0.72	-	0.76	37	0.186	5.4
125	1.28	20.1	0.17	0.76	-	0.87	41	0.194	4.7
130	1.48	23.2	0.20	0.81	-	0.98	45	0.200	4.0
135	1.72	27.0	0.23	0.86	-	1.11	50	0.208	3.4
140	2.00	31.4	0.27	0.91	-	1.26	56	0.216	3.0
145	2.32	36.4	0.31	0.97	-	1.42	62	0.223	2.5
150	2.70	42.4	0.36	1.03	-	1.61	69	0.231	2.2
155	3.14	49.3	0.42	1.09	-	1.83	77	0.238	1.9
160	3.65	57.3	0.49	1.16	-	2.07	86	0.245	1.6
165	4.24	66.6	0.57	1.23	-	2.35	95	0.251	1.4
170	4.92	77.2	0.66	1.31	-	2.66	106	0.257	1.2
175	5.72	89.8	0.77	1.39	-	3.01	117	0.263	1.0
180	6.64	104.2	0.90	1.48	-	3.41	130	0.267	0.9
185	7.72	121.2	1.04	1.57	-	3.87	145	0.272	0.8
190	8.97	140.8	1.21	1.66	-	4.39	161	0.275	0.7
195	10.42	163.6	1.41	1.77	-	4.97	178	0.278	0.6
200	12.10	190.0	1.63	1.88	0.07	5.63	198	0.279	0.5
205	14.06	220.7	1.90	1.99	0.10	6.38	219	0.280	0.41
210	16.34	256.5	2.20	2.12	0.25	7.23	243	0.279	0.36
215	18.98	298.0	2.56	2.25	0.34	8.19	270	0.278	0.31
220	22.05	346.2	2.98	2.38	0.42	9.28	300	0.288	0.26
225	25.62	402.2	3.46	2.53	0.52	10.52	332	0.293	0.23
230	29.77	467.4	4.02	2.69	0.62	11.92	369	0.297	0.20
235	34.59	543.1	4.67	2.86	0.73	13.51	409	0.300	0.17
240	40.18	630.8	5.42	3.03	0.83	15.30	453	0.301	0.14
245	46.69	733.0	6.31	3.22	0.94	17.34	503	0.301	0.12
250	54.24	851.6	7.32	3.42	1.06	19.65	558	0.300	0.11
255	58.55	Steady state wood crib burning					630		
260	58.55						632		
265	58.55						634		
270	58.55						636		
275	58.55						638		
280	58.55						640		
285	58.55						642		
290	58.55						644		
295	58.55						646		
300	58.55						648		

Table E2. Room Smoke Filling Time Predictions, Steady State Fires

Time (s)	Heat Release Rate 0.5 kW Smoke layer height (m)	Heat Release Rate 1.0 kW Smoke layer height (m)	Heat Release Rate 10 kW Smoke layer height (m)	Heat Release Rate 100 kW Smoke layer height (m)
0	0.00	0.00	0.00	0.00
2	2.38	2.37	2.34	2.27
4	2.35	2.34	2.28	2.15
6	2.33	2.32	2.22	2.04
8	2.31	2.29	2.17	1.95
10	2.29	2.26	2.12	
12	2.27	2.24	2.07	Note:1.99(m)
14	2.25	2.21	2.02	Reached
16	2.23	2.19	1.97	@ 7(s)
18	2.21	2.16		
20	2.19	2.14	Note:1.99(m)	
22	2.17	2.11	Reached	
24	2.15	2.09	@ 15(s)	
26	2.13	2.07		
28	2.11	2.04		
30	2.09	2.02		
32	2.07	2.00		
34	2.06	1.98		
36	2.04			
38	2.02	Note: 1.99(m)		
40	2.00	Reached		
42	1.99	@ 33(s)		

Table E3. Summary of Critical Event Predictions

Event	Time (s)	Velocity (m/s)
Smoke filling of room	~10-35	
Visibility of 1(m) in corridor	~175	
Smoke filling of corridor	~181	
Occurence of flashover	~245	
Ventilation limit in room	~250	
Smoke front velocity with ΔT of 10°C		0.44
Smoke transport time to near end of corridor	~ 9.5	
Smoke transport time to far end of corridor	~35.9	

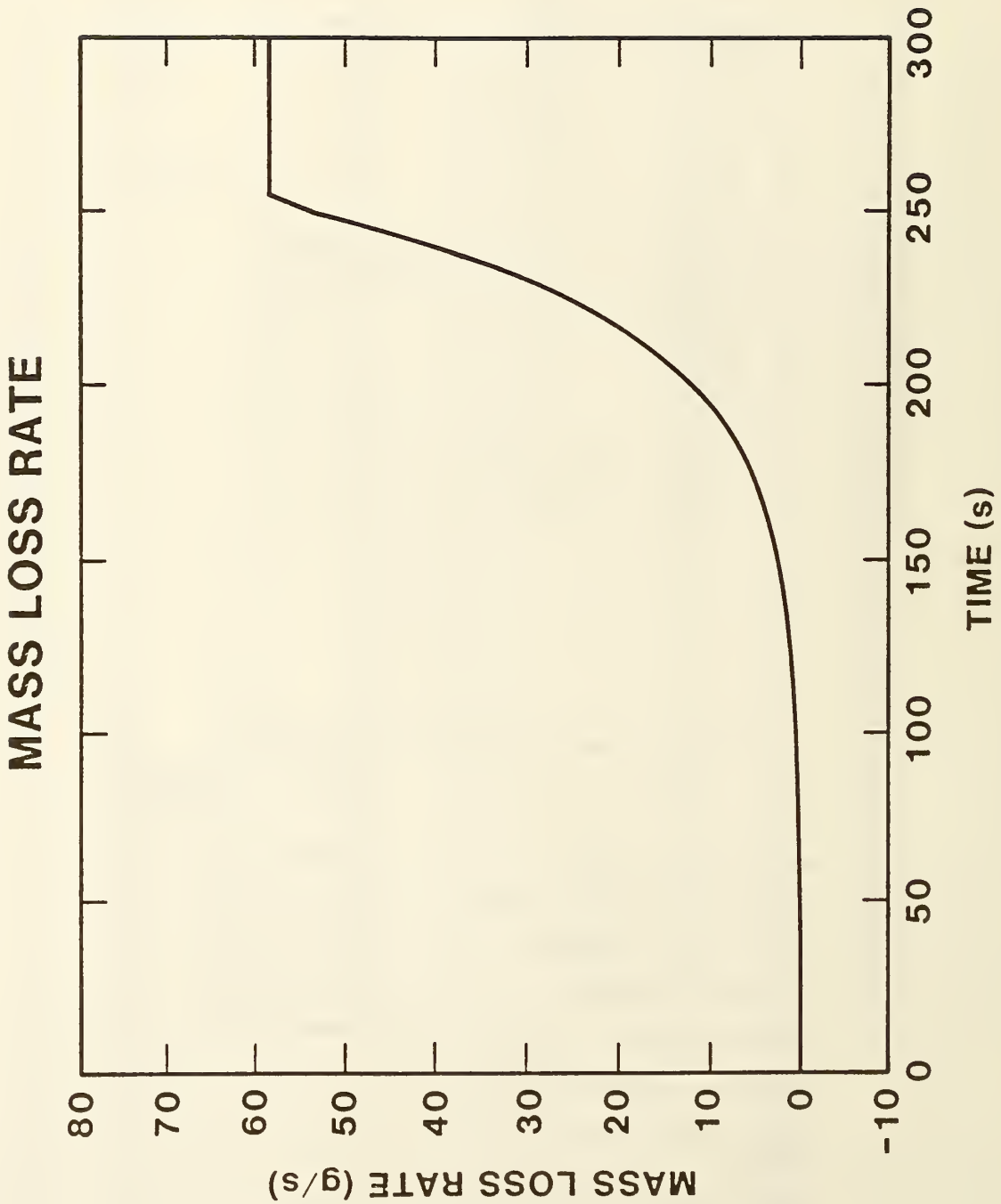

Figure E2. Mass Loss Rate for Fire Growth Example.

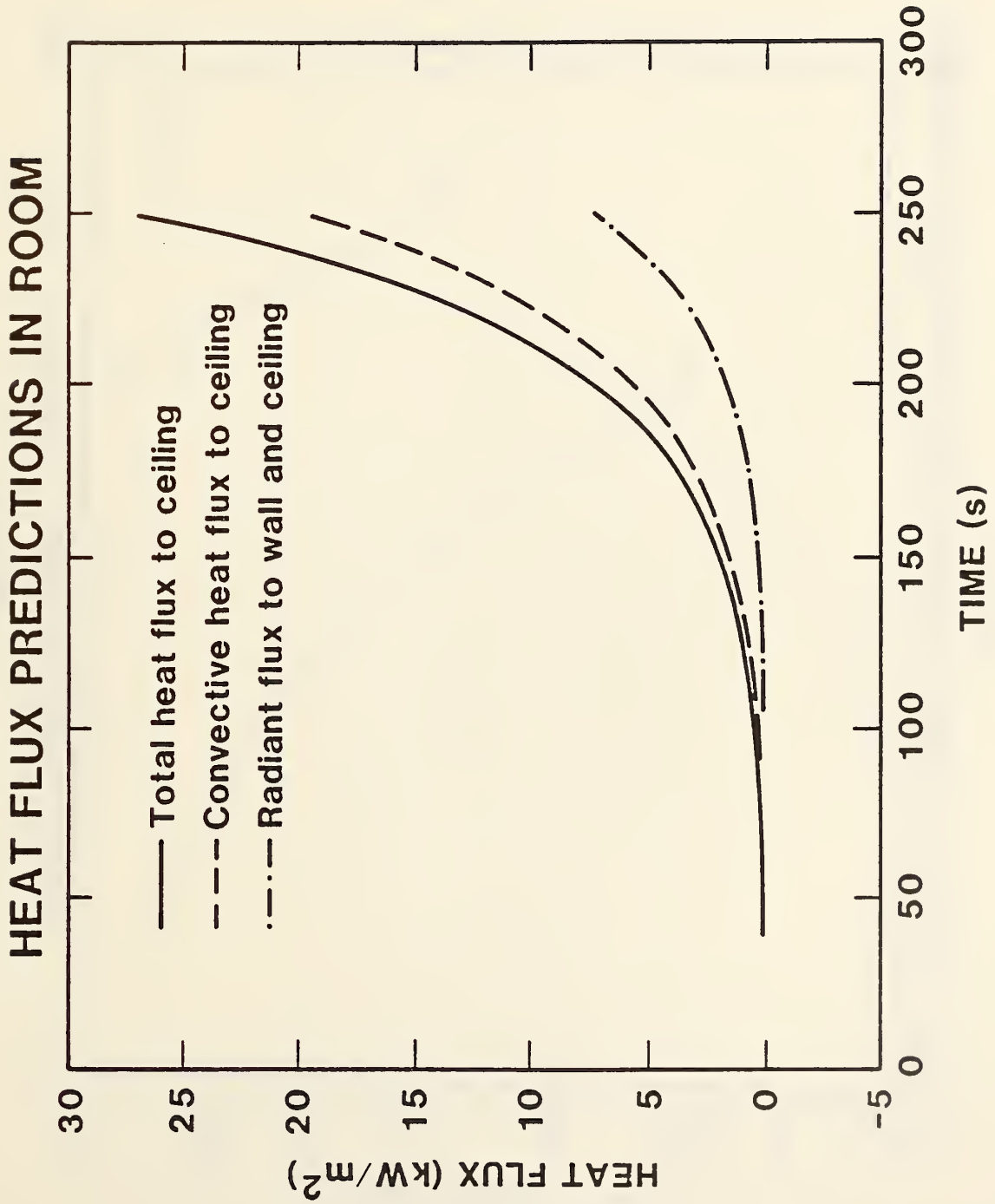

Figure E3. Heat Flux Predictions in Room for Fire Growth Example.

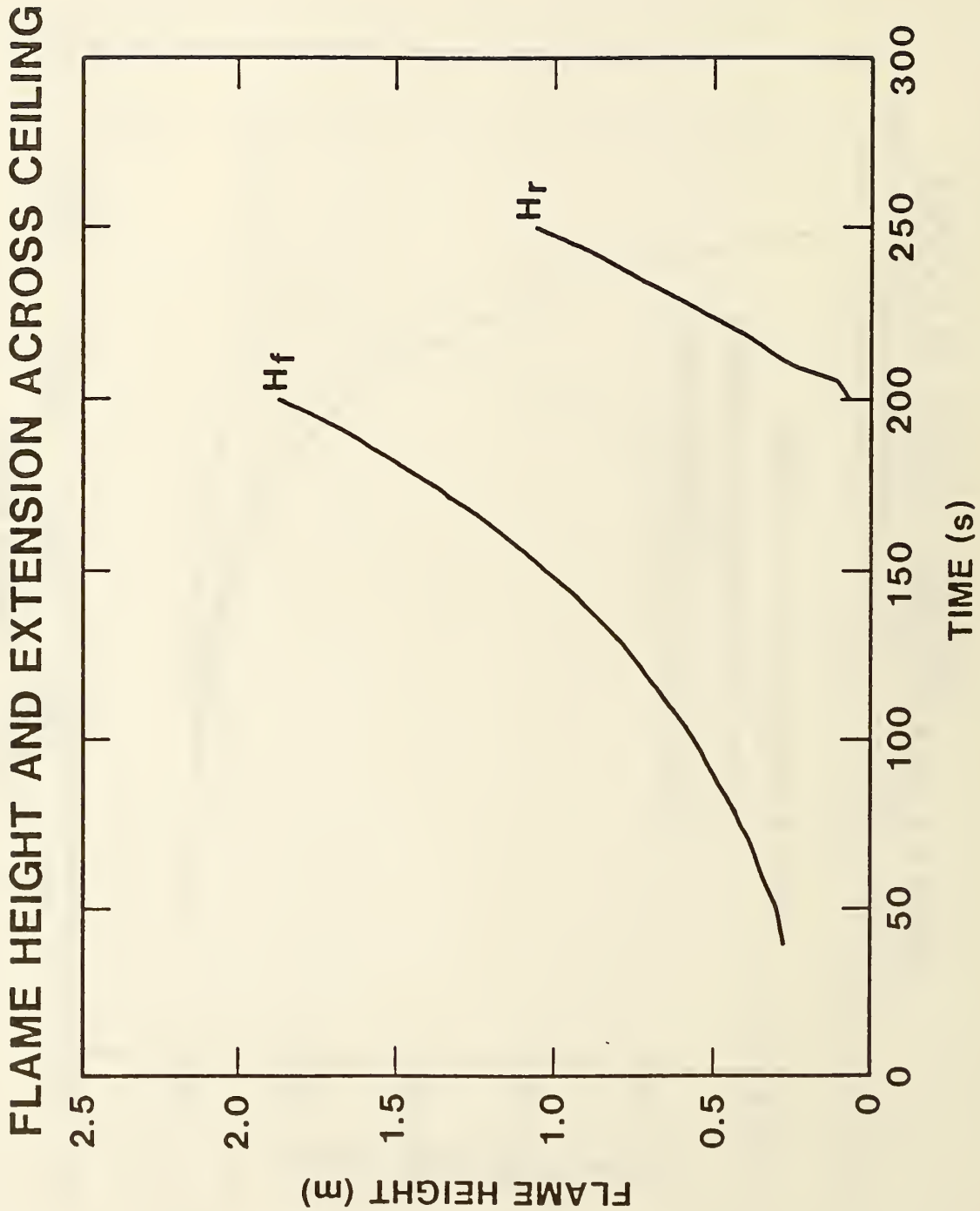

Figure E4. Flame Height and Extension Across Ceiling for Fire Growth Example.

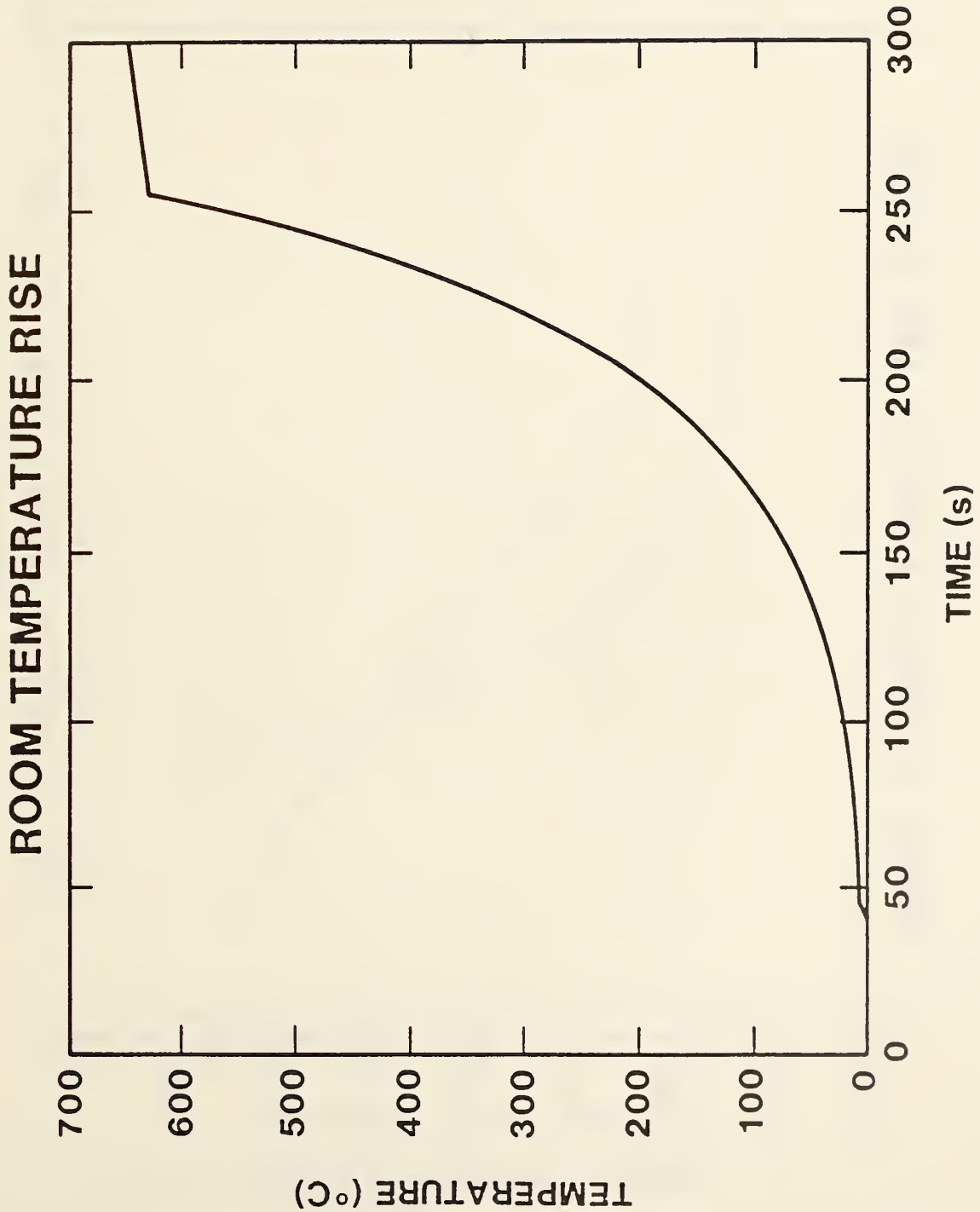

Figure E5. Room Temperature Rise for Fire Growth Example.

Figure E6. Mass Flow Rate into the Room for Fire Growth Example.

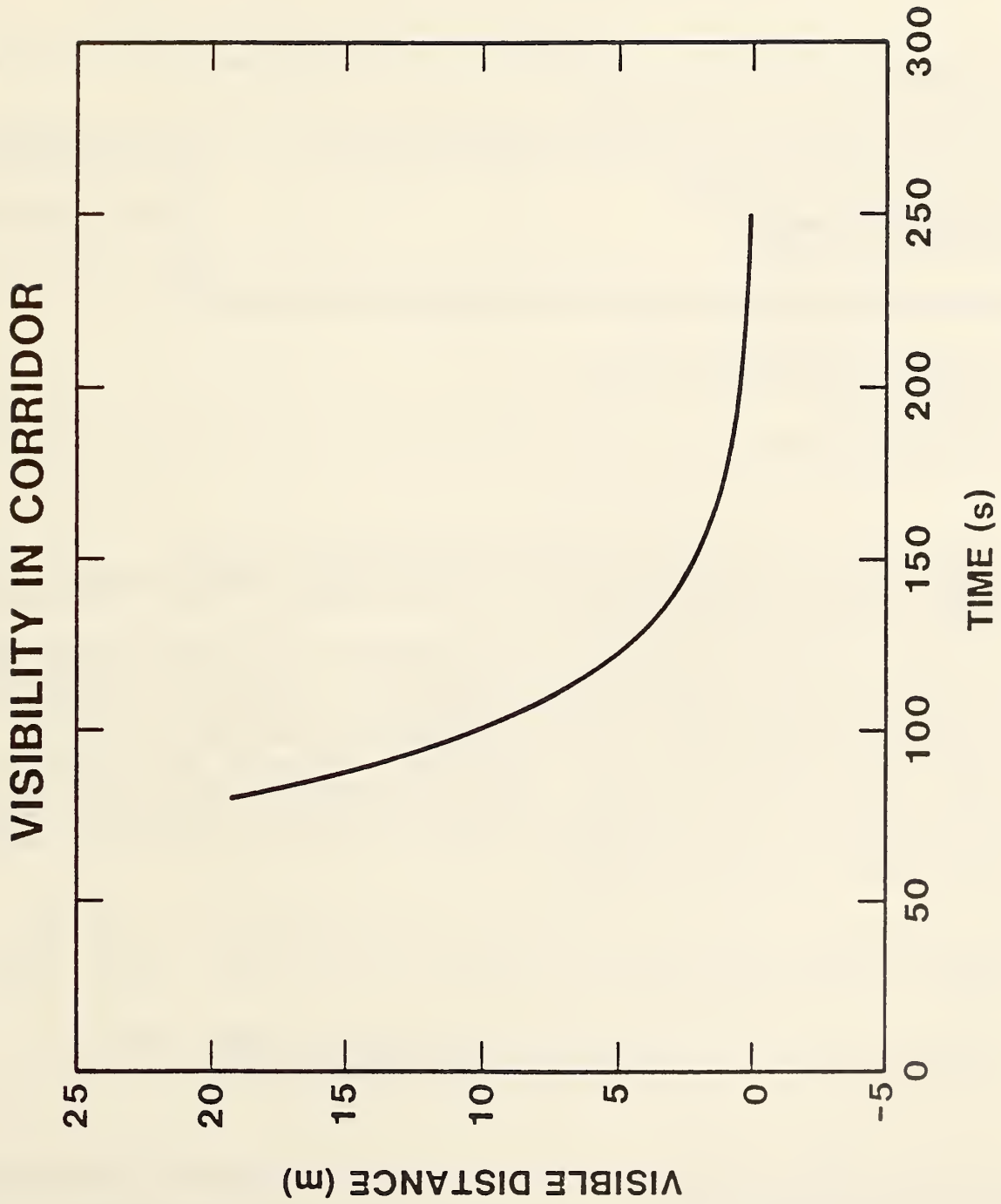

Figure E7. Visibility in Corridor for Fire Growth Example.

NBS-114A (REV. 2-8C)

U.S. DEPT. OF COMM. BIBLIOGRAPHIC DATA SHEET (See instructions)	1. PUBLICATION OR REPORT NO. NBSIR-85/3196	2. Performing Organ. Report No.	3. Publication Date June 1985

4. TITLE AND SUBTITLE

Slide-Rule Estimates of Fire Growth

5. AUTHOR(S)

J.R. Lawson and J. G. Quintiere

6. PERFORMING ORGANIZATION (If joint or other than NBS, see instructions)

NATIONAL BUREAU OF STANDARDS
DEPARTMENT OF COMMERCE
WASHINGTON, D.C. 20234

7. Contract/Grant No.

8. Type of Report & Period Covered

9. SPONSORING ORGANIZATION NAME AND COMPLETE ADDRESS (Street, City, State, ZIP)

U.S. David Taylor Naval Ship
Research and Development Center
Washington, D.C.

10. SUPPLEMENTARY NOTES

[ ] Document describes a computer program; SF-185, FIPS Software Summary, is attached.

11. ABSTRACT (A 200-word or less factual summary of most significant information. If document includes a significant bibliography or literature survey, mention it here)

A series of prediction methods have been assembled to provide an analytical basis for estimating fire growth in compartments. Solutions for each prediction method can be made using programmable scientific calculators. Prediction methods are presented for: fire size and growth rates, mass loss rates, radiant heat flux, flame height, radial flame impingement, heat flux to a ceiling, smoke filling of a room, carbon monoxide hazard with smoldering fires, temperature rise in a compartment, ventilation flow rate, flashover occurrence, corridor smoke transfer and filling, smoke concentration, visibility, flame spread rates, and fire burn time.

These predictive methods are useful for estimating many of the critical elements related to fire behavior and help provide a better understanding of this complex phenomenon.

This report appears in Appendix B in Fire Growth in Combat Ships by J.G. Quintiere, H.R. Baum and J.R. Lawson, NBSIR 85-3159.

12. KEY WORDS (Six to twelve entries; alphabetical order; capitalize only proper names; and separate key words by semicolons)

Calculators; computer programs; fire growth; fire models; room fires.

13. AVAILABILITY

[X] Unlimited

[ ] For Official Distribution. Do Not Release to NTIS

[ ] Order From Superintendent of Documents, U.S. Government Printing Office, Washington, D.C. 20402.

[X] Order From National Technical Information Service (NTIS), Springfield, VA. 22161

14. NO. OF PRINTED PAGES

56

15. Price

$10.00